Mapping of Genes Involved in Inherited Eye Disorders

By

Asima Zia

Department of Biochemistry
Quaid-I-Azam University
Islamabad

Mapping of Genes Involved in Inherited Eye Disorders

A thesis submitted in partial fulfillment of the requirements for the degree

of

Master of philosophy in

Biochemistry/Molecular Biology

By

Asima Zia

Department of Biochemistry
Quaid-I-Azam University
Islamabad

CERTIFICATE

The Department of Biochemistry, Faculty of Biological Sciences Quaid-i-Azam University Islamabad, accepts this thesis submitted by **Ms Asima Zia** in its present form, as satisfying the thesis requirements for the degree of Master of Philosophy in Biochemistry/Molecular Biology.

Supervisor: _____

Dr. Muhammad Ansar

External Examiner: _____

Dr. Mahmood A. Kayani

Chairman: _____

Dr. Wasim Ahmad

Dated: Feb 09, 2009

DECLARATION

I hereby declare that the work presented in the following thesis is my own effort and that the thesis is my own composition. No part of the thesis has been previously presented for any other degree.

Asima Zia

CONTENTS

LIST OF ABBREVIATIONS

µg	Microgram
µl	Micro liter
µM	Micro molar
aa	Amino acid
ABCR	ATP Binding cassette Transporter-retinol
adCRD	Autosomal dominant CRD
adRP	Autosomal dominant retinitis pigmentosa
AIPL1	Aryl hydrocarbon receptor-interacting protein 1
AMD	Age-related macular degeneration
AP	Ammonium persulphate
arCRD	Autosomal recessive CRD
arRP	Autosomal recessive retinitis pigmentosa
C- Terminus	Carboxyl terminus
CERKL	Ceramide kinase
cGMP	Cyclic guanosine monophosphate
cM	centi Morgan
CNGA1	Cyclic Nucleotide Gated Channel Protein Alpha 1
CNGA3	Cyclic Nucleotide Gated Channel Protein Alpha 3
CNGB1	Cyclic Nucleotide Gated Channel Protein Beta 1
CNGB3	Cyclic Nucleotide Gated Channel Protein Beta 3

CORDX	X-linked cone-rod dystrophy
CRALBP	Cellular retinaldehyde binding protein
CRB1	Crumbs Homolog 1 Beta
CRD	Cone-rod dystrophy
CRX	Cone-rod homeobox
DNA	Deoxiribonucleic acid
dNTP	Deoxiribonucleotide triphosphate
EDTA	Ethylene-diamine-tetra-acetic acid
GNAT	Glucosaminide acetyltransferas
GTP	Gaunosine triphosphate
GUCA1A	Guanylate cyclase activator 1A
GUCA1B	Guanylate Cyclase Activator 1B
GUCY2D	Retinal-specific guanylate cyclase
HCL	Hydrochloric acid
IMPDH1	Inosine Monophosphate Dehydrogenase Protein 1
kb	Kilobases
KCl	Potassium chloride
KDa	Kilo Dalton
LCA	Leber congenital amaurosis
LCA5	Lebercilin
LOD	Logrithims of odd
LRAT	Lecithin retinol Acyltransferase

M	Molarity
mA	Milliamphere
Mb	Megabases
MERTK	c-mer proto-oncogene Receptor Tyrosine Kinase
$MgCl_2$	Magnesium chloride
ml	Milliliter
mM	Milli molar
mRNA	Messenger RNA
N- Terminus	Amino terminus
Na^+	Sodium
NaCl	Sodium chloride
ng	Nanogram
NR2E3	Nuclear receptor Subfamily 2 group E3
NRE	NRL Response Element
NRL	Neural retina Leucine zipper protein
^oC	Degree centigrade
PAGE	Polyacrylamide gel electrophoresis
PCR	Polymerase chain reaction
PDE	Photodiesterase
PDE6A	cGMP Photoditerase 6 Alpha
PDE6B	cGMP Photoditerase 6 Beta

LIST OF TABLES

LIST OF FIGURES

INTRODUCTION

The development and function of an organism is in large part controlled by genes. Mutations, a permanent change in the DNA sequence that makes up a gene, can lead to changes in the structure of an encoded protein or to a decrease or complete loss in its expression. Because a change in the DNA sequence affects all copies of the encoded protein, mutations can be particularly damaging to a cell or organism (Lodish *et al.*, 2002). Mutations range in size from a single base to a large segment of a chromosome. Mutations that are passed from parent to child are called hereditary mutations or germline mutations and can be responsible for inherited disorders.

Recent advances in molecular genetics have made it possible to identify and isolate genes responsible for human diseases (Farber *et al.*, 1991). Genetic disorders are more common in consanguineous marriages because individuals born of consanguineous union have segments of their genomes that are homozygous as a result of inheriting identical ancestral genomic segments through both parents. One consequence of this is an increased incidence of recessive disease within these sibships (Woods *et al.*, 2006).

Hereditary visual deficiencies can result from isolated or associated alterations of any structure of the eye. The identification of the molecular basis of ophthalmological disorders has revived interest in several conditions forgotten since their original description and allowed the development of specific therapeutic projects (Kaplan and Rozet, 2006).

Taking into account the highly complex and sophisticated structure of the eye, it is not surprising that the eye is one of the most common sites of genetic diseases (Gregory-Evans and Bhattacharya, 1998). Eye diseases, which lead to blindness, remain a highly prevalent and serious health problem in many developing countries. The control of blindness in children is a priority because it affects their development, education and employment opportunities. This has far-reaching impact on the quality of not only their lives but also that of their families. According to a population-based survey 1987-1990, conducted by the Ministry of Health of Pakistan and the World Health Organization (WHO), Pakistan has 1.78% prevalence of blindness. In Pakistan, so far there is no

reported data available on prevalent causes of childhood blindness for any future recommendations. Reliable prevalence data are difficult to obtain for a variety of reasons but the available evidence suggests that the prevalence varies from 0.3/1000 children in economically developed countries to over 1.0/1000 children in underdeveloped societies (Khan *et al.*, 2007). The estimated blind adults in Pakistan are 1,140,000 (962,000–1,330,000) with 46.2% male and 53.9% female. Overall percentage of blindness is 0.8-1.0% in Pakistan being highest in the province of Punjab and Baluchistan (3.8%) while lowest in NWFP (2.6%) (Jadoon *et al.*, 2006).

The mature eye is a complex organ that develops through a highly organized process during embryogenesis. Alterations in its genetic programming can lead to severe disorders that become apparent at birth or shortly afterwards; for example, one-half of the cases of blindness in children have a genetic cause (Graw, 2003). Hereditary retinal diseases represent a broad range of retinal dysfunction and/or degeneration including retinitis pigmentosa (RP), cone or cone-rod dystrophy, Leber congenital amaurosis, congenital stationary night blindness (CSNB), color blindness, pathologic myopia, macular degeneration, retinoschisis, and chorioretinal atrophy. Over one hundred genes have been reported to be associated with these diseases (Zhang *et al.*, 2005a).

The Human Eye

Eyes are the organs that detect light and able to focus near and far objects to produce high resolution images. The average newborn's eyeball is about 18 millimeters in diameter, from front to back (axial length). The eye continues to grow, gradually, to a length of about 24-25 millimeters, or about 1 inch, in adulthood. The eyeball is set in a protective cone-shaped cavity in the skull called the "orbit" or "socket." This bony orbit also enlarges as the eye grows (Montgomery, 2008).

Structure of Eye

The orbit is surrounded by layers of soft, fatty tissue. These layers protect the eye and enable it to turn easily. Traversing the fatty tissue are three pairs of extraocular muscles, which regulate the motion of each eye: the medial & lateral rectus muscles, the superior & inferior rectus muscles, and the superior & inferior oblique muscles. The most

important anatomical components are the cornea, conjunctiva, iris, crystalline lens, vitreous humor, retina, macula, optic nerve, and extra-ocular muscles (Fig 1.1; Montgomery, 2008).

The Retina

The retina is an exquisitely delicate diaphanous membrane of neuro-ectodermal origin and is made up of a single layer of cuboidal cells: the retinal pigment epithelium (RPE) and a three layered neurosensory retina. The neurosensory retina is made up of rods and cone photoreceptors in the outer layer adjacent to the RPE with outer segments. The bipolar, amacrine, horizontal and Müller cells reside in the middle layer and ganglion cells form the inner layer (Koenekoop, 2004). The optic disc, where ganglion cell axons exit the eye to form the optic nerve, does not contain any photoreceptors, and is therefore also referred to as "the blind spot" (Awater *et al.*, 2005).

Photoreceptors

There are two types of photoreceptors in the human retina, rods and cones. Rods and cones have the same basic structure: an outer segment and an inner segment connected by a narrow connecting cilium (Fig 1.2). The outer segments face the RPE and contain stacks of membrane disks filled with visual pigments. The visual pigments consist of a protein part, opsin, and a vitamin A derived chromophore, retinal. The visual pigment in rod photoreceptors is rhodopsin (Hargrave *et al.*, 1983).

Rods are responsible for vision at low light levels (scotopic vision). They do not mediate color vision, and have a low spatial acuity. Cones are active at higher light levels (photopic vision), are capable of color vision and are responsible for high spatial acuity. There are 3 types of cones, which are referred to as the short-wavelength sensitive cones (S-cones), the middle-wavelength sensitive cones (M-cones) and the long-wavelength sensitive cones (L-cones) (Fig 1.2; Wikipedia, www.wikipedia.org).

Visual Cycle in Rods

In the retina, photoreceptor cells convert light energy into an electrical signal through a phototransduction process that consists of an enzymatic cascade, and is similar for rods

and cones, but the details are better worked out in rods (Koenekoop, 2004). Vision in all species begins with the absorption of light by rhodopsin; initiating the heterotrimeric G-proteins mediated phototransduction cascade in retinal rod discs of the eyes. This cascade is also known as the Visual Cycle or Visual Signal Transduction. The signaling cascade responsible for sensing light in vertebrates is initiated by rhodopsin in discs of rod cells (Thompson and Gal, 2003). High cGMP levels keep cGMP-gated ion channels in the open state and allow them to pass an inward Na^+ current. Phototransduction involves three main biochemical events:

- Light entering the eye activates the opsin molecules in the photoreceptors
- Activated rhodopsin causes a reduction in the cGMP intracellular concentration
- The photoreceptor is hyperpolarized following exposure to light

The phototransduction cascade can be amplified and later on terminated by employing several mechanisms which ensure the proper functioning of the photoreceptor cells (Clandinin, 2006). The importance of these processes in evident from the involvement of many genes at these levels and mutations in these can result in many inherited retinal disorders.

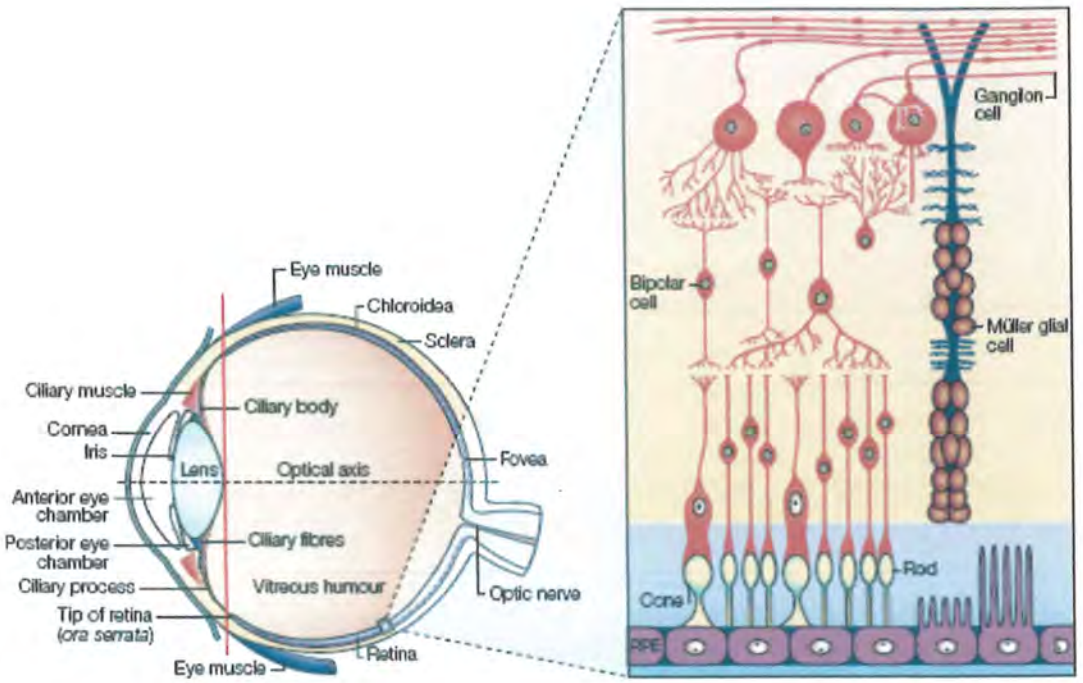

Figure 1.1 Schematic section through an adult human eye. This illustration shows the main tissues of the human eye. The vertical line divides the anterior segment of the eye (the Cornea, Lens, Iris and Ciliary Body) from the posterior segment (consisting mainly of the Vitreous humour, Retina, and the Choridea). Light enters the eye through the cornea, the anterior chamber and the lens. Before it meets the retina, light has to pass through the vitreous humour. The panel on the right shows a close-up view of the components of the retina, which are (from the outside to the inside of the retina): the retinal pigmented epithelium (RPE), photoreceptor cells (rod and cone), Müller Glial cells, bipolar cells and Ganglion cells (Adapted from Graw, 2003).

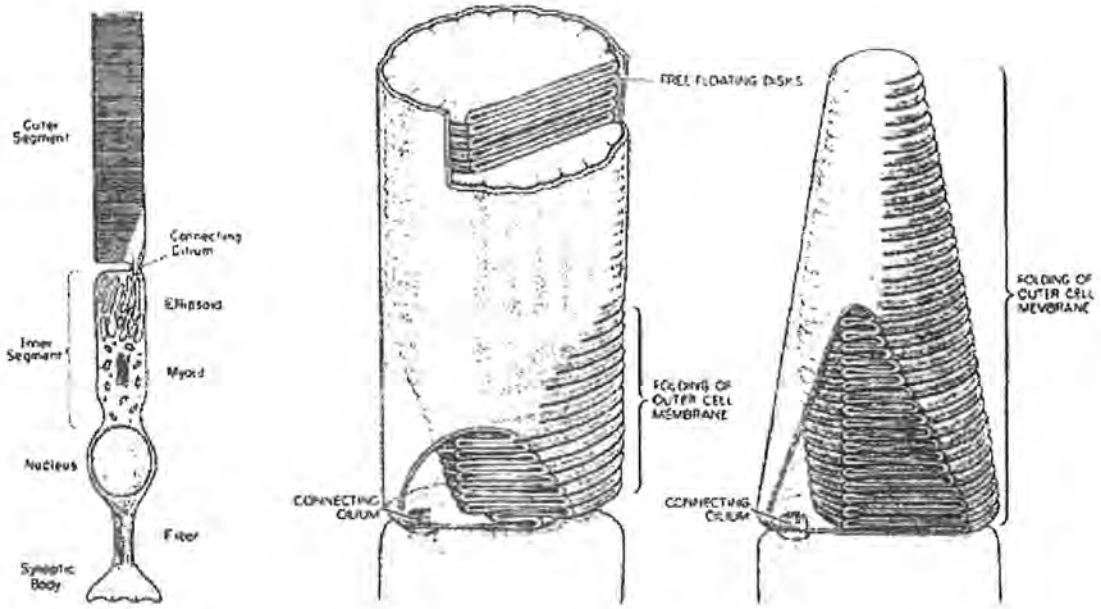

Figure 1.2 Schematic diagram of structure of rods and cone. At the left is a generalized conception of the important structural features of a vertebrate photoreceptor cell. At the right, are shown the differences between the structure of rod (left) and cone (right) outer segments (Adapted from Wikipedia, the free encyclopedia, 2008).

Inherited Retinal Degenerations

Inherited diseases that cause the retina to degenerate, leading to either partial or total blindness, affect approximately 1 in 3000 people. Rapid progress is being made in identifying the genetic causes of common, inherited retinal diseases, such as retinitis pigmentosa and macular degeneration, as well as some of the rare forms of retinal disease (Sullivan and Daiger, 1996). To date, nearly 200 mapped loci, including 138 cloned genes for inherited retinal diseases, have been identified (Retinal Information Network, RetNet, www.sph.uth.tmc.edu/Retnet/home.htm). Human retinal dystrophies and dysfunctions are a common group of inherited retinal diseases that are genetically complex, and exhibit significant clinical overlap between the different types. Retinal dystrophies lead to photoreceptor death or dysfunction and blindness with a profound impact on the individual and society, as the blindness is lifelong and currently irreversible. A growing body of data suggests that genetic factors also play a role in the development of the most common retinal disease (Patel *et al.*, 2007).

The mode of inheritance can be autosomal dominant or recessive, X-linked dominant or recessive, digenic, mitochondrial, or complex. The genes associated with inherited retinal diseases are involved in many different cellular processes and functions, including visual transduction, retinoid cycle, regulation of gene expression, splicing, cellular trafficking, and metabolic and structural functions (Gregory-Evans and Bhattacharya 1998; Maubaret and Hamel 2005; Travis *et al.*, 2007). The majority of the genes are retina-specific or retina-enriched, but ubiquitously expressed genes may also cause "pure" retinal phenotypes (Blackshaw *et al.*, 2001). In some cases, even genes that are not expressed in the retina may cause a retinal phenotype, as in the case of retinol binding protein, RBP4, which delivers retinol from the liver stores to the peripheral tissues (Seeliger *et al.*, 1999).

A striking feature in retinal diseases is the involvement of exceptional genetic, allelic, and clinical heterogeneity. Mutations in many different genes may cause the same disease, while different mutations in the same gene may cause different diseases. Furthermore, clinical features may be variable even among family members who carry the same mutation (Sullivan and Daiger, 1996). An example of heterogeneity is retinitis

X-Linked RP (XLRP)

X-linked retinitis pigmentosa (XLRP) is a severe progressive retinal degeneration which affects about 1 in 25,000 of the population (Meindl *et al.*, 1996). X-linked RP can be either recessive, affecting males only, or dominant, affecting both males and females; females are always mildly affected (Pagon and Daiger, 2005). So far, 4 loci and 2 genes have been identified for XLRP which include RP6, RP23, RP24, RP34 and RP2, RPGR respectively.

Linkage studies have suggested that the RP GTPase-regulator (RPGR) gene accounts for 70% to 90% of XLRP. More than 300 RPGR mutations have been reported, which are associated with X-linked retinitis pigmentosa, cone-rod dystrophy, or atrophic macular atrophy, and syndromal retinal dystrophies with ciliary dyskinesia and hearing loss. All disease-causing mutations occur in one or more RPGR isoforms containing the carboxyl-terminal exon open reading frame 15 (ORF15) (Shu *et al.*, 2007). The prevalence of disease-causing mutations in other associated genes is either lower or unknown (Wang *et al.*, 2005b). RP2 mutations cause disease in approximately 15% of XLRP families (Zito *et al.*, 2003).

Autosomal Dominant RP (adRP)

Autosomal dominant RP (adRP) accounts for 15-20% of all cases of RP (Wang *et al.*, 2005a; Riazuddin *et al.*, 2006). To date 17 genes and one loci have been identified including CA4, CRX, FSCN2, GUCA1B, IMPDH1, NR2E3, NRL, PRPF3, PRPF8, PRPF31, PRPH2, RHO, ROM1, RP1, RP9, SEMA4A, TOPORS and RP33 respectively (Retinal Information Network, RetNet, www.sph.uth.tmc.edu/Retnet/home.htm).

Mutations of the RHO gene and the RP1 gene occur in approximately 30% of patients with adRP (Wang *et al.*, 2005b). More than 100 RHO mutations have been reported but one, P23H, with distinct sectorial disease, is found in approximately 10% of Americans affected with adRP. Mutation of IMPDH1, RP1 and PRPF31 accounts for 3-5%, 5-10% and 15-20% of adRP cases respectively. The prevalence of mutations in remaining genes

are either rare or unknown (Pagon and Daiger, 2005). The severe form of adRP is caused by mutation in PRPF8 gene (Walia *et al.*, 2008).

Autosomal Recessive RP (arRP)

Autosomal recessive retinitis pigmentosa (ARRP) is also genetically heterogeneous disorder (Hmani-Aifa *et al.*, 2008). Autosomal recessive RP (arRP) is the most common form of RP worldwide (Riuz *et al.*, 1998) and accounts for around 20% of all cases of RP, while sporadic RP accounts for a further 50%. Mutations causing autosomal recessive RP (arRP) have been found in the genes encoding rhodopsin, the α and β subunits of rod phosphodiesterase, the α subunit of the cyclic GMP gated channel protein, and the genes RPE65, RLBP1, ABCR, and TULP1 (Bessant *et al.*, 2000). Most of the arRP genes are rare, causing 1% or fewer cases, but RPE65 (expressed in the RPE), PDE6A and PDE6B (phosphodiesterase subunits in the phototransduction cascade), cause 2-5% of cases; mutations in USH2A, which can also cause Usher syndrome, may account for up to 5% of arRP cases (Table 1.2; Pagon and Daiger, 2005).

Genes that are associated with other forms of retinitis pigmentosa may also be associated with autosomal recessive retinitis pigmentosa one such gene is RP1. RP1 mutations that are associated with autosomal dominant retinitis pigmentosa also cause recessive retinitis pigmentosa. Like mutations in MERTK, a member of the MER/AXL/TYRO3 receptor kinase family, have been associated with disruption of the Retinal Pigment Epithelium (RPE) phagocytosis pathway and settling of autosomal recessive RP (arRP) in humans (Brea-Fernández *et al.*, 2008).

Riuz *et al.*, (1998) identified a new locus for arRP, on chromosome 6, between markers D6S257 and D6S1644 and named as RP26. A novel gene encoding a ceramide kinase (CERKL), which encompassed 13 exons, was finally identified in locus RP26 (Tuson *et al.*, 2004).

Table 1.1: Genes Causing Autosomal Recessive RP (arRP) (in Chromosomal Order) adapted from Pagon and Daiger (2005)

Locus Name	Gene Symbol	Locus	Percent of arRP
RP20/LCA2	*RPE65*	1p31	2%
RP19	*ABCA4*	1p21-p13	~5% [2]
RP12	*CRB1*	1q31-q32.1	Rare
	USH2A	1q41	4-5%
RP28	Unknown	2p15-p11	One family
	MERTK	2q14.1	Rare
RP26	*CERKL*	2q31.2-q32.3	Rare
	SAG	2q37.1	Rare
RP4	*RHO*	3q21-q24	Rare
CSNB3	*PDE6B*	4p16.3	3-4%
	CNGA1	4p12-cen	Rare
RP29	Unknown	4q32-q34	Rare; 4 families
	LRAT	4q31	Unknown
	PDE6A	5q31.2-q34	3-4%
RP14	*TULP1*	6p21.3	Rare
RP25	Unknown	6q14-q21	10-20% of arRP in Spain
	RGR	10q23	Unknown
RP27	*NRL*	14q11.1-q11.2	Unknown
	NR2E3	15q23	Rare; found in Sephardic Jews in Portugal
	RLBP1	15q26	Unknown
RP22	Unknown	16p12.3-p12.1	Rare
	CNGB1	16q13	Unknown

1. CSNB= congenital stationary night blindness
2. LCA= Leber congenital amaurosis
3. RP= Retinitis pigmentosa

2004) and 1/81,000 (Stone, 2007) but it is thought to account for 5% of inherited retinal disease (Leroy and Dharmaraj, 2003).

Clinical Description

LCA is characterized by following four clinical features: severe and early visual loss, sensory nystagmus, amaurotic pupils and absent electrical signals on electroretinogram (ERG) (den Hollander *et al.*, 2008). LCA presents very early in life, usually at around the age of 6 weeks, when parents note the oscillations of the eyes (nystagmus) or the absence of fixation (Koenekoop, 2004).

Genetics of LCA

LCA is a clinically and genetically heterogeneous (multigenic) disorder (Zernant *et al.*, 2005; Seong *et al.*, 2008). LCA is inherited as an autosomal recessive trait in the large majority of patients, with only a limited number of cases with autosomal dominant inheritance described (Leroy and Dharmaraj, 2003). Dominantly inherited LCA has been associated with a 12-bp deletion in the CRX gene (Sohocki *et al.*, 1998). To date 14 genes mutated in patients with LCA and juvenile retinal degenerations have been identified (den Hollander *et al.*, 2008) including GUCY2D, CRB1, RPGRIP1, CRX, RDH12, IMPDH1, CEP290, AIPL1, RPE65, MERTK, LCA5, RD3 while LRAT and TULP1 have also been implicated in LCA (Mataftsi *et al.*, 2007; den Hollander *et al.*, 2008).

Together, mutations in these 14 genes account for approximately 70% of all LCA cases. CEP290 (15%), GUCY2D (12%) and CRB1 (10%) are the most frequently mutated LCA genes (Fig 1.4). The LCA genes encode proteins with a wide variety of retinal functions, such as photoreceptor morphogenesis (CRB1, CRX), phototransduction (AIPL1, CUCY2D), vitamin A cycling (LRAT, RDH12, RPE65), guanine synthesis (IMPDH1), and outer segment phagocytosis (MERTK) (den Hollander *et al.*, 2008).

LCA Genes and Loci

The first disease causing gene, LCA1, mapped to chromosome 17p13 was discovered in 1996 (Perrault *et al.*, 1999). To date, more than 400 mutations have been identified in the

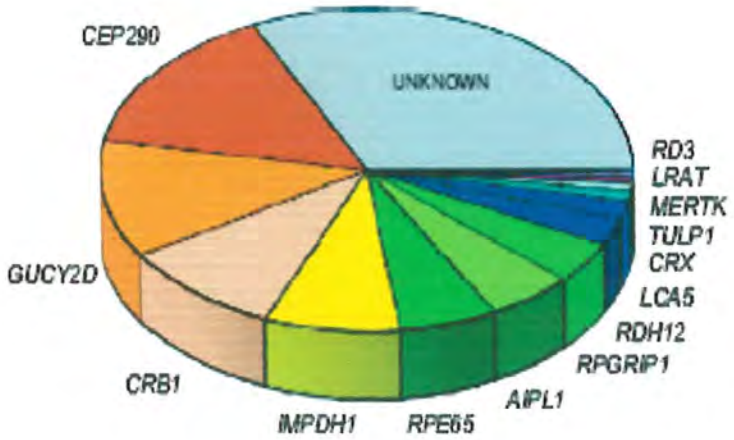

Figure 1.4: Prevalence of LCA-associated mutations for the 14 causative genes. CEP290 (15%), GUCY2D (12%) and CRB1 (10%) are the most frequently mutated genes. Mutations in approximately 30% of all cases remain to be identified (Adapted from den Hollander *et al.*, 2008).

Retinoid Cycle (RPE65, RDH12, LRAT)

Retinal Pigment Epithelium 65 (RPE65)

The RPE65 gene (chromosome 1p31) encodes an abundant and evolutionarily conserved 533-amino acid (65-kD) protein that is peripherally associated with the RPE smooth endoplasmic reticulum (Thompson and Gal, 2003), that is a key component of the visual cycle (Bainbridge *et al.*, 2008; den Hollander *et al.*, 2008). Mutations in the RPE65 gene appear to account for 2% of cases of recessive RP and 16% of cases of LCA (Morimura, 1998; Weleber *et al.*, 2006). Since the identification of RPE65 as the first RPE specific disease gene, nearly 60 different disease associated RPE65 mutations have been described (Lorenz *et al.*, 2000; Lotery *et al.*, 2000; Dharmaraj *et al.*, 2000; Simovich *et al.*, 2001). Chen *et al.* (2006) identified single point mutations that altered subcellular localization of RPE65 and abolished its isomerohydrolase activity leading to vision loss in LCA patients (Chen *et al.* 2006).

Retinol Dehydrogenase 12 (RDH12)

RDH12 is a member of a subfamily of four retinol dehydrogenases (RDH11-14). RDH12 is expressed in the mouse and human photoreceptor inner segments (den Hollander *et al.*, 2008). Mutations in RDH12 account for ~4% cases of LCA (Weleber *et al.*, 2006). Although RDH12 lies 8 Mb from LCA3, it has conclusively been shown to be separate from the LCA3 locus (Thompson *et al.*, 2005). The most frequent sequence variant is a frameshift deletion in exon 6, 806-810del5 (Weleber *et al.*, 2006).

Lecithin Retinol Acyltransferase (LRAT)

LRAT is a 230-aa polypeptide (26 kD) that catalyzes the synthesis of retinyl esters and plays an essential role in the regeneration of visual chromophore and metabolism of vitamin A. LRAT is localized to the membrane of the endoplasmic reticulum and assumes a single membrane-spanning topology with an N-terminal cytoplasmic/C-terminal luminal orientation (Golczak *et al.*, 2005; den Hollander *et al.*, 2008). Thompson *et al.*, (2001) identified disease-associated mutations (S175R and 396delAA) in LRAT gene in individuals with severe, early-onset disease (Thompson *et al.*, 2001).

Photoreceptor Development and Structure (CRB1, CRX)

Crumbs Homologue 1 (CRB1)

CRB1 is homologous to the Drosophila transmembrane protein Crumbs. Drosophila Crumbs is required for maintenance of apico-basal cell polarity and adherens junction in embryonic epithelia, and has a similar function in adult fly retina (den Hollander *et al.*, 2008). The CRB1 protein is involved in photoreceptor development and structure (Yzer *et al.*, 2006). Crumbs molecules are found in many species, ranging from invertebrates to mammals (den Hollander *et al.*, 2008). Mutations in CRB1 account for 5-15% cases of LCA (Weleber *et al.*, 2006). Coding sequence variations in the CRB1 gene occur more frequently than in any of the other LCA associated genes (Lotery *et al.*, 2001). Vallespin *et al.*, (2007) identified that CRB1 is the main gene responsible for LCA in the Spanish population (Vallespin *et al.*, 2007).

Cone-Rod Homeobox (CRX)

The Cone-rod homeobox gene CRX is a member of the highly conserved orthodenticle-related (otx) gene family, and encodes a 299-aa homeobox transcription factor with a predicted mass of 32 kDa (den Hollander *et al.*, 2008). The CRX gene has 3 exons and mutations in CRX account for ~3% cases of LCA (Weleber *et al.*, 2006). The mutations that result in CRX protein with reduced DNA binding and transcriptional regulatory activity (like R90W) lead to very early onset severe visual impairment in LCA (Swaroop *et al.*, 1999).

Transport across the Photoreceptor Connecting Cilium

(RPGRIP1, TULP1, CEP290, Lebercilin)

Retinitis Pigmentosa GTPase Regulator Interacting Protein (RPGRIP1)

The RP GTPase regulator interacting protein 1 (RPGRIP1) directly binds to the RP GTPase regulator (RPGR) with its C-terminal RPGR interacting domain (RID). LCA associated mutations in the RID of RPGRIP1 could lead to a gain and loss-of-binding to RPGR (den Hollander *et al.*, 2008). Mutations in RPGRIP1 account for ~5% cases of LCA (Weleber *et al.*, 2006). Gerber *et al.*, (2001) identified eight distinct mutations

among which the most common type of mutation was truncating (Gerber *et al.*, 2001). Dryja *et al.*, (2001) also identified null mutations creating premature termination codons resulting in degeneration of both rod and cone photoreceptors (Dryja *et al.*, 2001).

Tubby-Like Protein 1 (TULP1)

TULP1 is a member of the Tubby-like protein (TULP) family, consisting of 4 proteins in vertebrates (TUB, TULP1-3). TULP1 gene encodes a 542-aa (61kDa) protein that plays an important role in the development and function of the central nervous system (den Hollander *et al.*, 2008). Mutations in TULP1 have been associated with LCA and considered as a rare cause of LCA with only 14 mutations reported so far. The observed intrafamilial phenotypic variability could be attributed to disease progression or possibly modifier alleles (Weleber *et al.*, 2006; Mataftsi *et al.*, 2007).

Lebercilin (LCA5)

Lebercilin (6q11-q13) was first reported by Camuzat *et al.*, (1995) a gene for LCA to the distal short arm of chromosome 17 by linkage analysis. The LCA5 gene is almost ubiquitously expressed during early embryonic development, while at later stages its expression shifts towards ciliated tissues (den Hollander *et al.*, 2007). The LCA5 gene product is a 677-aa (100 kDa) protein lebercilin (den Hollander *et al.*, 2008) and localizes to the connecting cilia of photoreceptors and to the microtubules, centrioles and primary cilia of cultured mammalian cells (den Hollander *et al.*, 2007). So far only two reports have been made for LCA5 mutations causing LCA which are nonsense, frameshift and missense mutations of the LCA5 gene (den Hollander *et al.*, 2007; Ramprasad *et al.*, 2008).

CEP290

CEP290 is a novel centrosomal protein that was first described in association with RD 16 in the mouse. Mutations in CEP290 account for 10-20% cases of LCA. Mutations of CEP290 also cause Joubert syndrome (Weleber *et al.*, 2006) an autosomal recessive disorder characterized by neurological features, including psychomotor delay, hypotonia, and ataxia (den Hollander *et al.*, 2006). Cremers *et al.*, (2002) have reported that CEP290

accounts for a substantial percentage of individuals with LCA. den Hollander *et al.*, (2006) reported that intronic mutation (c.2991+1655ArG) that creates a strong splice-donor site and inserts a cryptic exon in the CEP290 messenger RNA causes LCA.

LCA in Pakistan

Hameed *et al.*, (2000) studied a two-generation consanguineous Pakistani family and identified autosomal recessive Leber congenital amaurosis (LCA, MIM 204,000) and keratoconus and suggested that this combined phenotype maps to a new locus and is due to yet uncharacterized gene within the 17p13 chromosomal region. Jabeen *et al.*, (2005) suggested that AIPL1 is the candidate gene, which is involved in the pathogenesis of autosomal recessive Leber congenital amaurosis and found significant linkage for marker D17S796 at LCA4 locus (17p13.1) in a Pakistani consanguineous kindred. AIPL1 mutations were found to cause LCA in Pakistani families and p.Trp278X mutation accounts for approximately half of all AIPL1 alleles, and may represent a founder mutation in the Pakistani population (Sohocki *et al.*, 2000a, b). Jalali *et al.*, (2005) carried out linkage analysis in a five-generation Pakistani consanguineous family suffering from LCA and found linkage with LCA4 locus (17p13.1) (Jalali *et al.*, 2005). Khaliq *et al.*, (2002) carried out linkage analysis in a Pakistani family and mapped the disease locus on chromosome 17p 13.1. They identified a novel homozygous C to A transversion in exon 2 at nucleotide 116. This mutation alters the codon 39 for threonine to asparagine (Khaliq *et al.*, 2002).

Linkage to the LCA5 locus has also been reported in a consanguineous family from Pakistan. den Hollander *et al.*, (2007) detected homozygous nonsense and frameshift mutations in LCA5 in two of the five families he studied (den Hollander *et al.*, 2007). Keen *et al.*, (2003) identified a new locus, LCA9, on chromosome 1p36, at which the disease segregates in a single consanguineous Pakistani family. They carried out whole genome search and identified an autozygous region of 10 cM between the markers D1S1612 and D1S228. This region contains 50 distinct genes and one of these retinoid binding protein 7 (RBP7), was screened for mutations but no mutation was found (Keen *et al.*, 2003).

Clinicians and scientists continue to reveal the relationship between phenotype and genotype in hereditary retinal diseases. Persistent investigation and progressive technology are advancing the efficiency of mutation discovery. This technology is also leading to readily available genetic testing that aids clinicians in the diagnosis of these diseases. Functional genetic studies, laboratory and human clinical trials are occurring that may lead to future treatment of these disorders (Goodwin, 2008).

The work presented here involves linkage analysis in two Pakistani families with inherited eye disorders. The families will be tested for linkage to the known loci responsible for inherited congenital dystrophies.

MATERIALS AND METHODS

Families Studied

Two families referred as family 'A' and family 'B' showing autosomal recessive eye disorder residing in different regions of Pakistan were recruited for the present study. The case history, number of affected individuals, number of generations involved, onset of eye defects were carefully noted. All the information obtained was cross checked by interviewing different persons. Special attention was paid to consanguineous marriages and deceased persons. The phenotypes of affected persons mentioned in the pedigree were recorded for clinical diagnosis of the disorders. One affected individual from each family (A and B) was clinically examined by local ophthalmologist for phenotype characterization. Blood samples from affected and normal individuals of each family were collected for DNA extraction.

Pedigree Analysis

Pedigree is the most important step while studying human genetic disorder. This helps geneticists to infer the mode of inheritance of the trait. For genetic inference an extensive pedigree was constructed for each family by the standard methods described by Bennett *et al.*, (1995). The exact genealogical relationships for all the affected individuals were obtained through extensive personal interviews of elders of the families. Males were symbolized by squares and females by circles. The filled circles or squares were indicative of affected individuals. Each generation was denoted by Roman numeral while the individuals within a generation were designated by Arabic numerals. Double lines in the pedigree represent the consanguineous marriages. The segregation or transmission of the disorder within a family was deduced by observing the pattern of inheritance of eye disorder and was expressed in the form of pedigree.

Blood Sampling

The blood samples from both affected and normal members of the families including their parents were collected by using 10 ml clean and sterilized syringes (0.8 x 38 mm 21_G x 1 $^{1/2}$) and from children below 2 years of age by butterflies in standard potassium

EDTA vacutainer tubes. Blood samples were then processed for genomic DNA extraction.

Extraction and Purification of Human Genomic DNA from Blood

Two methods were used for the extraction and purification of the Human Genomic DNA from venous blood samples:

- Organic preparation using 1.5 ml microcentrifuge tubes
- Commercially available kit

Organic preparation using 1.5 ml micro centrifuge tubes

Organic (Phenol- Chloroform) method was used for the extraction and purification of the genomic DNA from blood samples. Approximately 0.75 ml of blood was taken in a 1.5 ml microcentrifuge tube and mixed with equal volume of solution A and was kept at room temperature for 5-10 minutes. The tube was then centrifuged at 13,000 rpm for 1 minute in a Microcentrifuge (Eppendorf 5417 C. Germany). Supernatant was discarded and pellet was resuspended in a 400 µl of solution A. Centrifugation was done again, and after discarding the supernatant, nuclear pellet was resuspended in 400 µl of solution B, 12 µl of 20% SDS and 5 µl Proteinase K (20mg/ml stock concentration) and incubated at 37°C overnight. On the following day 0.5 ml of fresh mixture of equal volume of solution C and solution D was added in samples, mixed and centrifuged for 10 minutes at 13,000 rpm. The aqueous phase (upper layer) was shifted into a new microcentrifuge tube and equal volume of solution D was added. Centrifugation was then carried out again at 13,000 rpm for 10 minutes. The aqueous phase (upper layer) was shifted into a new tube, and after adding 55µl of 3M sodium acetate (pH 6) and equal volume of isopropanol, the tubes were gently inverted several times to precipitate DNA and centrifuged at 13,000rpm to settle DNA. The supernatant was discarded and the DNA pellet was washed with 70% chilled ethanol and dried at room temperature for 8-10 minutes. After evaporation of residual ethanol, DNA was dissolved in an appropriate amount (150-200µl) of Tris EDTA.

Composition of Solutions

Solution A

0.32 M Sucrose

10 mM Tris pH 7.5

5 mM $MgCl_2$

1 % v /v Triton X-100

Solution B

10 mM Tris (pH 7.5)

400 mM NaCl

10 mM Tris (pH 8.0)

Solution C

Phenol

10 mM Tris (pH 8.0)

Soution D

Chloroform (24 volume)

Isoamyl alcohol (1 volume)

Tris-EDTA (TE) Buffer

10 mM Tris (pH 8.0)

0.1 mM EDTA

DNA Extraction by Commercially Available Kit

DNA extraction was also carried out by Kit (PureGene USA). Approximately 150µl of whole blood was taken in 1.5 ml eppendorf tube and 450µl of RBC lysis solution was added. The tube was then incubated for 1 min with mixing for 10 times during incubation. The tube was then centrifuged for 20 seconds at 13,000-16,000 rpm. Supernatant was discarded and was vortexed vigorously for 10 sec to resuspend the white

blood cells. 150µl of cell lysis solution was added to resuspend the pellet and vortexed several times. Then sample was placed on ice for 1 min and 50µl of protein precipitation solution was added and vortexed vigorously at high speed for 20 sec. Then centrifuged at 13,000-16,000 rpm for 1 min and supernatant was transferred to 1.5 ml microfuge tube containing 150µl of 100% propanol. Then centrifuged at 13,000-16,000 rpm for 1 min and supernatant was discarded and 150 µl of 70% ethanol was added to wash the pellet. Again centrifuged at 13,000-16,000 rpm for 1 min and the pellet was air dried for 5 sec and 50 µl of DNA hydration solution was added. DNA samples were incubated at room temperature for overnight and stored at 4 °C for further processing.

Horizontal Gel Electrophoresis

Genomic DNA was analyzed on 1% agarose gel, prepared by melting 0.4 g agarose in 40ml 1X TBE (0.89M Tris-Borate, 0.025M EDTA) in a microwave oven for 1 minute. 5 µl of ethidium bromide (final concentration 0.5 µg/ml) was added to visualize the stained DNA after electrophoresis.

Five µl of genomic DNA samples were mixed with loading dye (0.25% bromophenol blue with 40% sucrose) and samples were loaded into the wells. Electrophoresis was performed at 100 volts (80 mA) for half an hour in 1X TBE running buffer. After analyzing genomic DNA on agarose gel dilutions were made.

Polymerase Chain Reaction (PCR)

Polymerase Chain Reaction was performed in 0.2 ml tubes (Axygen, USA) containing 25 µl total reaction mixture. The reaction mixture was prepared by adding 1µl sample DNA (40 ng), 2.5 µl of 10X PCR buffer (KCl 500 mM, Tris-HCl 100 mM, pH 8.3), 1.5 µl 25 mM $MgCl_2$ with 0.5 µl dNTPs (10 mM), 0.3 µl of each forward and reverse microsatellite marker (0.1 µM), one unit Taq DNA polymerase (MBI Fermentas, Sunderland, UK), in 18.4 µl PCR water. The reaction mixture was vortexed and centrifuged for few seconds for thorough mixing. Reactions were performed by means of T1 thermocyclers (Biometra, Germany) and Gene Amp 9700 (Applied Biosystems, USA). The conditions were set as, an initial denaturation of template DNA at 95°C for 5 min, followed by 40

cycles of amplification each consisting of 3 steps: denaturation at 95°C for 1 min, annealing or hybridization of microsatellite markers to their complementary sequences at 55-57°C for 1 min, and elongation at 72°C for 1 minute. The final elongation by Taq DNA polymerase to synthesize any unextended strand was carried out at 72°C for 10 minutes.

Agarose Gel Electrophoresis

The amplified PCR products of DNA samples were analyzed on 2% agarose gel, which was prepared by melting 1 gram of agarose in 50ml 1 X TBE buffer (0.89 M Tris-Borate, 0.032 M EDTA pH 8.3) in a microwave oven for two minutes. Ethidium bromide (final concentration 0.5 μg/ml) was added to visualize the stained DNA after electrophoresis.

Five μl of PCR products were mixed with loading dye (0.25% bromophenol blue with 40% sucrose) and samples were loaded into the wells. Electrophoresis was performed at 100 volts (80 mA) for half an hour in 1X TBE running buffer. Amplified products were visualized by placing the gel on SynGene gel documentation system (Synoptics Ltd, England), images were taken using Gene Snap (Version 7.04.05) and later on the gel images were analyzed using Gene Tools (Version 3.08.03).

Polyacrylamide Gel Electrophoresis

The amplified PCR products were resolved on 8% non-denaturing polyacrylamide gel. Gel solution was made in a 250 ml conical flask, and was poured in a space between the two glass plates separated at a distance of 1.5 mm. After placing the comb, the gel was allowed to polymerize for 45-60 minutes at room temperature. Samples were mixed with loading dye (0.25% bromophenol blue with 40% sucrose) and loaded into the wells. Electrophoresis was performed in a vertical gel tank of GIBCO V16-2 (GIBCO BRL, USA) at 100 volts (80 mA) for 90-100 minutes depending upon the size of amplified product. The gel was stained with ethidium bromide solution (final concentration 0.5 μg/ml) and visualized on SynGene gel documentation system (Synoptics Ltd, England).

Composition of 8% Polyacrylamide Gel (50 ml)

13.5 ml 30% Acrylamide solution (29 g acrylamide, 1g N, N Methylene-bis-acrylamide).

5 ml of 10X TBE

350 µl of 10% Ammonium persulphate (AP)

17.5 µl of TEMED (N, N, N', N'- Tetra methyl ethylene diamine)

31.13 ml distilled water

Genotyping

The analysis of the microsatellite markers was performed by PCR, and the amplified products were resolved on 8% standard non-denaturing polyacrylamide gel as described above. Microsatellite markers were visualized by placing the ethidium bromide stained gel on SynGene gel documentation system. The images were captured with digital camera (Syngene, USA) and were analyzed for allele scoring. Microsatellite markers mapped by Cooperative Human linkage Center (CHLC) were obtained from Gene Link (USA) and Alpha DNA (Canada). The cytogenetic location of these markers as well as the length of amplified products was obtained from genome data base homepage (www.gdb.org) and rutgers combined linkage-physical human genome map (Kong *et al.*, 2004).

Linkage Studies

Linkage to Known Congenital Eye Disorders Loci

In the present study several candidate loci were tested for linkage by typing microsatellite markers linked to loci for congenital inherited eye disorders. Table 2.1 summarizes microsatellite markers used for exclusion mapping of known autosomal recessive loci for congenital eye disorders.

Linkage to other known Loci for inherited eye disorders

After exclusion of linkage to loci for congenital eye disorders, additional loci for inherited eye disorders were screened for linkage to find causative gene/loci. Table 2.2 summarizes microsatellite markers located in the region of these loci (for inherited eye disorders). These markers were also genotyped as described above.

Linkage and Haplotype Analysis

After genotyping of the families with microsatellite markers summarized in Table 2.1 and 2.2 alleles were scored for each of them by analysis of images acquired by documentation system. Then marker files (Annexure I) were created for each microsatellite marker in easyLINKAGE plus Version 5.0 format (Linder and Hoffmann, 2005). Pedigree files (Annexure II) were created in linkage format and data was checked for genotyping errors and Mendelian inconsistencies using the PEDCHECK software (O'Connell *et al.*, 1998) incorporated in easyLINKAGE plus Version 5.0. Two point linkage analyses were performed for each marker by SUPERLINK, version 1.5 (Feshelson *et al.*, 2002) with map distances from Marshfield genetic map (Broman *et al.*, 1998). The disease assumed to be autosomal recessive with a disease-allele frequency 0.001. For linkage analysis equal allele frequencies were used for all genotyped markers.

Sequencing

Amplification PCR

For sequencing first amplification PCR was performed in 0.2 ml tubes (Axygen, USA) containing 50 µl total reaction mixture. The reaction mixture was prepared by adding 2 µl sample DNA (40 ng), 5 µl of 10X PCR buffer (KCl 500 mM, Tris-HCl 100 mM, pH 8.3), 3 µl 25 mM $MgCl_2$ with 1 µl dNTPs (10 mM), 0.6 µl of each forward and reverse microsatellite marker (0.1 µM), one unit Taq DNA polymerase (MBI Fermentas, Sunderland, UK), in 36.8 µl PCR water. The reaction mixture was vortexed and centrifuged for few seconds for thorough mixing. Reactions were performed by means of T1 thermocyclers (Biometra, Germany) and Gene Amp 9700 (Applied Biosystems, USA). The conditions were set as described above. Amplified PCR product was visualized on 2% agarose gel for non-specificity and band intensity. Then amplified PCR product was purified using Rapid PCR Purification kit (Marligen, USA).

Purification of PCR product

400 µl of binding solution (H1) (concentrated Guanidine HCl, EDTA, Tris-HCl, and isopropanol) was added to the amplification reaction and mixed thoroughly. Vortexed

and loaded on the cartridge in a wash tube, centrifuged at 13,000 rpm for 1 min and discarded the flow through. Then washed the cartridge with 700 µl wash buffer (H2) (containing ethanol) and centrifuged at 13,000 rpm for 1 min. Again discarded the flow through and repeated the centrifugation step. Finally the cartridge was transferred to 1.5ml recovery tube and 35 µl of TE (Tris-EDTA buffer) preheated to 65 °C was added. Then incubated for 1 min at room temperature and centrifuged at 13,000 rpm for 2 min. Purified PCR product was visualized on 2% agarose gel for confirmation and band intensity.

Sequencing PCR

The reaction mixture was prepared by adding 3µl DTCS quick start kit (Beckman, UK), 1µl Sequencing buffer (CEQ8800 sequencing kit, Beckman, UK), 1 µl forward/reverse primer (0.1 µM) (Table 2.3 and 2.4), 1-2µl template (3-10ng) and 4-3µl PCR water. The reaction mixture was vortexed and centrifuged for few seconds for thorough mixing. Reactions were performed by means of T1 thermocycler (Biometra, Germany). The conditions were set as an initial denaturation of template DNA at 96°C for 1 min, followed by 30 cycles of amplification each consisting of 3 steps: denaturation at 96°C for 25 sec, annealing or hybridization of microsatellite markers to their complementary sequences at 55-57°C for 25 sec, and elongation at 60°C for 4 minute. The final extension was performed at 60°C for 10 minutes.

Ethanol Precipitation

The sequencing reaction was transferred to 1.5ml eppendorf and 2.5µl freshly prepared stop solution [1µl 3M sodium acetate (pH 5.2), 1µl 100mM sodium EDTA (pH 8.0) and 0.5µl Glycogen (20mg/ml)] and 70µl 100% ethanol (-20°C) was added. Then vortexed and centrifuged at 13,000 rpm for 20 min and immediately the supernatant was removed with P200 and 150 µl 70% ethanol (-20°C) was added and centrifugation step was repeated. Then supernatant was immediately removed and the pellet was dried at 30°C. Then the pellet was resuspended in 30 µl of sample loading solution (SLS). The samples were transferred to the sample plate (CEQ8800, Beckman, UK) and a drop of mineral oil

was added on each sample. The samples were then sequenced on automated DNA sequencer (CEQ8800, Beckman, UK).

Mutation Analysis

Using BioEdit software, version 7.0.9.0 (Hall, 1999) mutation analysis was carried out. The gene sequence was taken from Ensembl Gene Sequence view (http://www.ensembl.org/index.html). Data obtained was compared with gene sequence by aligning two sequences in BioEdit (Version 7.0.9.0) using ClustalW software to identify changes. Once a variation was identified in an affected individual, all the family members were screened to verify the pathogenic nature.

Table 2.1: List of microsatellite markers of known autosomal recessive loci for congenital eye disorders.

S.No.	Gene	Markers	Distance (cM)*
1	CNGB3	D8S1119 D8S1143 GATA8B01	96.45 Nil 99.15
2	CNGA3	D2S1258 D2S2972 D2S1343	Nil 116.19 117.62
3	GNAT2	GATA133A08Q D1S1627	133.63 134.13
4	AIPL1	D17S1298 GATA158H04	13.24 19.97
5	GUCY2D	D17S1353 D17S1805 D17S974	23.31 24.41 33.56
6	CRX	D19S559 D19S545 D19S596 D19S246	70.77 73.97 78.7 82.48
7	RDH12	D14S1069 D14S119 D14S554 D14S588	62.99 63.17 64.65 64.65
8	RPGRIP1	ATA251 D14S122 D14S742 D14S548	Nil 5.03 9.22 9.22

*Average-sex distance in cM according to Rutgers combined linkage-physical human genome map (Kong *et al.*, 2004).

Table 2.2: List of microsatellite markers for other inherited eye disorders

S. No.	Locus	Markers	Distance (cM)*	Gene
1	RP19	D1S1588 D1S406 D1S1587	122.02 122.31 126.2	ABCA4
2	RP26	D2S2261 D2S426 D2S425	188.07 192.53 196.39	CERKL
3	R1	D4S1627 D4S3241 D4S2300	65.85 66.1 Nil	KCTD8
4	R2	D16S526 D16S2620	78.66 82.53	CNGB1
5	RP12	D1S2625 D1S533 D1S1660	197.51 199.81 202.04	CRB1
6	R3	D4S1606 D4S3049 D4S413	152.47 156.8 160.3	LRAT
7	R4	D2S1888 D2S410 D2S2265	122.67 127.67 132.4	MERTK
8	R5	D15S1015 D15S650 D15S188	68.95 73.47 76.75	NR2E3
9	R6	D5S436 D5S2490 D5S812	150.91 143.55 155.39	PDE6A
10	R7	D4S3360 D4S432 D4S2285	0 5.72 7.97	PDE6B
11	R8	D10S523 D10S1174 D10S1658	105.84 104.31 105.38	RGR

Table 2.2: (Continued)

S. No.	Locus	Markers	Distance (cM)*	Gene
12	RP4	D3S3607 D3S2316 D3S1541	135.87 131.76 138.91	RP4
13	R9	D15S811 D15S652	87.35 98.56	RLBP1
14	R10	D1S1178 D1S1665 D1S2876	103.59 104.28 108.34	RPE65
15	R11	D2S2344 D2S2973	242.83 249.85	SAG
16	RP14	D6S1014 GATA129G03 D6S1051	Nil Nil 58.42	TULP1
17	R12	D1S2827 D1S2860	225.64 229.03	USH2A
18	RP28	D2S1337 S2S286	82.74 99.33	Unkown
19	RP29	D4S2290 D4S2431 GATA67A08	104.31 176.78 184.46	Unkown
20	RP25	D6S257 D6S1282 D6S1031	83.02 86.79 93.11	Unkown
21	RP22	D16S287 D16S420	38.49 48.71	Unkown

*Average-sex distance in cM according to Rutgers combined linkage-physical human genome map (Kong *et al.*, 2004).

Table 2.3: List of primers used for amplification and sequencing of AIPL1 gene

S No	Exon	Forward Primer	Reverse Primer	Tm	Product Size
1	1	CCTGGTCCCCTGTCTTCTT	TGTTGAAAGCTGCTGTGGGG	57°C	480bp
2	2	GGCCTTGAACAGTGTGTCTA	GAGCCCAGAAAAGACTAGTC	57°C	278bp
3	3	GGCCTTTTATGGCCCACCTA	CTGTCCCTCTCCAGTGCTGG	57°C	310bp
4	4	TATGCACTTGACCAGCAAGC	AGGGAGAAGGTCAGCCATGA	54°C	417bp
5	5	AAGTGGCGCTGACTCTGGGG	TGTCTCCGTGGCCCTGGGCT	57°C	299bp
6	6	GGATGGGGGATACAGAGAGG	AGGTGGCTCTGTGGATGACT	54°C	402bp

Table 2.4: List of primers used for amplification and sequencing of RGR gene

S No	Exon	Forward Primer	Reverse Primer	Tm	Product Size
1	1	ATTCCCCGACCTTAATCCTG	GTTTGGGGACCTCTCCTCTC	55°C	452bp
2	2	AGGTTGCTGATGTTCCATCC	CCCTTGGCCAATTTTCTGTA	55°C	364bp
3	3	CTCCAACGCCTCATAGGAAA	TGCATGCACACTCACACCTA	55°C	413bp
4	4	TATAGCCAGCACAGCCTCAA	GGAGTGGGAGAAGTGCTCTG	55°C	228bp
5	5	TATCAGGCCATCTCCTCCTC	GCCAAGATTCCCATGGATAG	55°C	255bp
6	6	TCATCTAGGGCAGAGCTGGT	TTTGTTCGGGACACCAAGAG	55°C	274bp
7	7	GCTGAGTGCTGACCTGGTTT	ACATGAGGTTTGGGCAATGT	55°C	424bp
8	8	CCATGCATCTCCACCAACTA	CAGGTCCATCTGGCTCTTTC	55°C	468bp
9	8A	GAAGGACCGAACCAAGTGAG	ACACGTGGACATGGAGTGTG	55°C	467bp
10	8B	AGAGGCCTCAGGAAAGTCATT	TGGTGATTTCTCCATACTGTCTTA	57°C	611bp
11	8C	TCATCTGTTGATGGATAGATTCC	TTGCAAACCATGTATCCAGAA	55°C	577bp
12	8D	GCTTCTTAGCCACGTGTATGTA	CTTCTGGGCATTGGTCTAGG	57°C	366bp

RESULTS

Description of the Families Studied

Family A

Family A demonstrates autosomal recessive congenital blindness. The pedigree drawing presented in Figure 3.1 indicates seven generations with 2 affected males (VI-7 and VII-5) and 5 affected females (V-5, V6, VI-1, VI-6 and VII-4). The pedigree analysis shows that affected individuals being produced by the unaffected parents and the affected status was independent of the sex suggesting that the trait is transmitted in autosomal recessive manner. The parents (IV-7 and IV-8), (V-1 and V-2), (V-3 and V-4) and (VI-8 and VI-9) are normal phenotypically but resulted in two (V-5 and V-6), one (VI-1), two (VI-6 and VI-7) and two (VII-4 and VII-5) affected children, respectively.

For linkage studies blood samples were collected from fifteen members of family A, including seven affected (V-5, V6, VI-1, VI-6, VI-7, VII-4 and VII-5) and eight normal (IV-7, V-3, V-4, VI-2, VI-5, VI-8, VI-9 and VII-3) individuals.

Family B

Family B also demonstrates autosomal recessive congenital blindness. The five-generation pedigree (Figure 3.2) contains 27 individuals including 1 affected male (V-5) and 4 affected females (IV-4, IV-5, V-2 and V-4). Pedigree analysis is suggestive of autosomal recessive mode of inheritance and consanguineous loops could account of all the affected persons being homozygous for an abnormal allele. All the affected persons have phenotypically normal parents but they carry the recessive allele in heterozygous condition.

The DNA was extracted from the blood samples collected from four affected individuals including one male (V-5) and three females (IV-4, IV-5 and V-4) along with six normal individuals (III-1, III-2, IV-6, IV-7, V-1 and V-3).

Clinical Description of Family A and B

One affected individual of each family (VI-7; Family A, V-5; Family B) was diagnosed by local ophthalmologist, which revealed that the affected individuals from both families had bilateral nystagmus. The clinical examination also revealed grossly normal retina but dull macular refraction in both eyes. This may indicate the segregation of cone dystrophy in these families. The affected individual of family A also exhibit photophobia and show excessive blinking in sunlight. The blinking was present since childhood but more frequent in elder affected individuals of family A. These affected individuals also experience pain in sunlight. Both families show no other associated disorders or symptoms like Usher syndrome, Bardet biedl syndrome, mental retardation, metabolic diseases or renal diseases suggesting that these families do not have any syndromic form of blindness.

Linkage Analysis

On the basis of genetic linkage studies in inherited eye disorders, it is clear that at least some candidate intervals should be tested for linkage or exclusion prior to embarking on genome-wide scan. In the present study, the two families (A and B) were tested for linkage to known loci including loci for congenital retinal disorders and RP by genotyping microsatellite markers mapped within the candidate linkage intervals (Table 2.1 and 2.2).

Family A

To identify the underlying gene in this family, linkage analysis was performed using the DNA samples of the seven individuals including four normal (V-3, V-4, VI-2 and VI-5) and three affected (VI-1, VI-6 and VI-7). The results of DNA analysis with polymorphic microsatellite markers revealed that affected individuals were heterozygous for these markers except GATA158H04 at chromosome 17 (Figure 3.3-3.19). Three affected individuals were homozygous (VI-1, VI-6 and VI-7) for GATA158H04, whereas the normal individuals were heterozygous for different alleles, thus indicate linkage to this marker (Figure 3.19a). In order to confirm linkage to this region, GATA158H04 and

three additional markers (D17S1298, D17S1805 and D17S974) were genotyped with all fifteen members of the family. The analysis of the results confirms linkage of family A to 17p13.1 region (Figure 3.18-3.21). After which haplotypes were formed (Figure 3.22) and LOD score was calculated using easyLINKAGE plus v5.08. LOD score for marker D17S1805 (Figure 3.20) and GATA158H04 was 1.7967 and 1.7896 respectively, whereas no other region produced significant LOD score (Figure 3.23). These LOD scores indicate that there is probability of disease gene linkage in this locus. This locus contains two genes AIPL1 and GUCY2D (Khaliq *et al.*, 2002). So mutation can be present in any one of these two genes.

Family B

In family B, nine DNA samples including five normal (III-1, III-2, IV-6, IV-7 and V-1) and four affected (IV-4, IV-5, V-4 and V-5) individuals were used for genotyping. Later on the sample IV-4 was not used because of less availability of DNA and was stored for linkage confirmation. The results of DNA analysis with polymorphic microsatellite markers revealed that heterozygosity in affected individuals with tested markers except two markers D10S523 and D10S1658 at chromosome 10 (Figure 3.24-3.66). In addition to D10S523 and D10S1658 two other markers D1S533 and D14S588 show homozygous alleles in three affected individuals only. Three affected individuals (IV-4, IV-5 and V-5) were homozygous for marker D1S533, while one affected individual (V-4) was heterozygous for parental alleles (Figure 3.31). Similarly three affected individuals (IV-5, V-4 and V-5) were homozygous for D14S588 but one affected individual (IV-4) was heterozygous and two normal individuals (III-1 and IV-6) were also homozygous (Figure 3.61). On further analysis with additional markers the linkage to markers D1S533 and D14S588 was ruled out. In case of D10S523 and D10S1658, all four affected (IV-4, V-3, V-4 and V-5) individuals were homozygous and normal individuals were heterozygous for different alleles, thus indicating linkage to these markers (Figure 3.65-3.66). In order to confirm linkage to this region four additional markers (D10S1765, D10S1143, D10S1687 and D10S1644) were genotyped. The analysis of the results confirms linkage of family B to 10q23.1 region (3.65-3.70). After which haplotypes were constructed (Figure 3.71) and LOD score was calculated using easyLINKAGE plus v5.08. LOD score

for markers D10S1658, D10S523 and D10S1765 was 1.1936, 0.4629 and 1.1117 respectively (Figure 3.72). These LOD scores indicate that there is probability of disease gene at this locus. This locus contains one gene RGR (RPE-retinal G protein-coupled receptor) and mutations of RGR gene are associated with retinitis pigmentosa (Fong *et al.*, 2006).

Mutation Screening

Family A

AIPL1 gene has six exons (ucsc genome browser, http://genome.ucsc.edu), and was sequenced from the DNA samples of the affected and normal individuals of family A. After sequencing the raw data was analyzed using BioEdit software. All exons sequenced were compared with the original sequence data from Ensembl genome browser (http://www.ensembl.org). Sequence analysis of all six exons revealed that AIPL1 gene in this case has no mutations but variations were present in exon 3 and 5 while in case of exon 1, 2, 4 and 6 no variations or polymorphism were observed. So the mutation may be present in the GUCY2D gene, as variations identified in AIPL1 gene are also present in normal individuals so these can not be associated with disease phenotype in family A.

Family B

Retinal G protein coupled receptor1 (RGR) gene has seven coding exons (ucsc genome browser, http://genome.ucsc.edu). Sequencing of four exons was carried out by using primers for these exons (Table 2.4) to find disease causing mutations. After sequencing exon sequence was analyzed using BioEdit (Version 7.0.9.0), which revealed that these exons 2, 3, 7 and 8 have no mutation and variation (Figure 3.73-3.74). Since no disease causing mutations are present in sequenced exons so remaining exons of this gene are needed to be sequenced for finding any disease associated mutation.

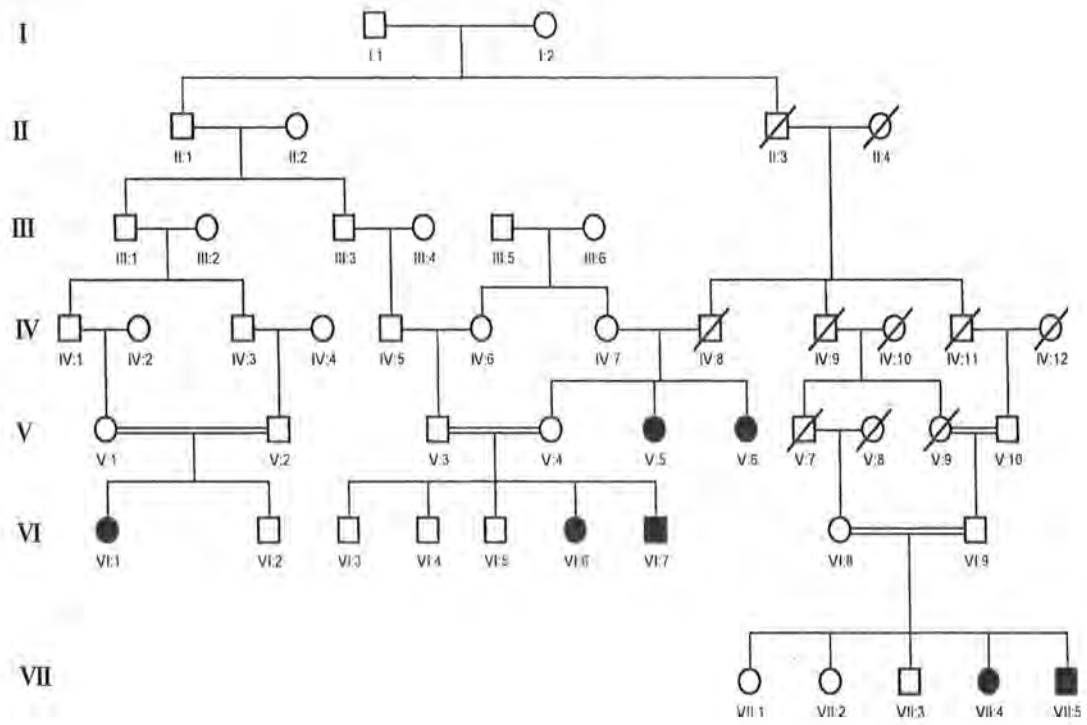

Figure 3.1: Pedigree of family A with inherited eye disorder. The pedigree shows the recessive mode of inheritance. Circles represent females and squares represent males. Filled circles and squares represent affected individuals. Double lines indicate consanguineous marriages. Cross lines on the symbols represent deceased individuals.

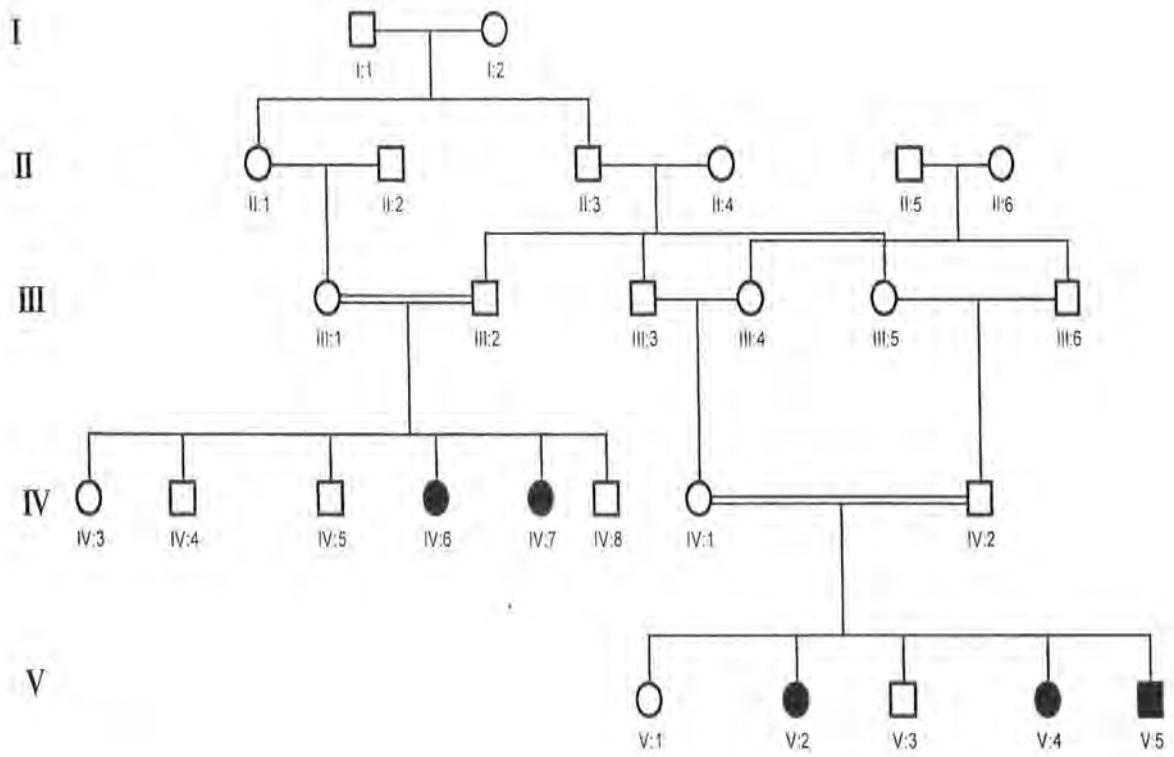

Figure 3.2: Pedigree of family B with inherited eye disorder. The pedigree shows the recessive mode of inheritance. Circles represent females and squares represent males. Filled circles and squares represent affected individuals. Double lines indicate consanguineous marriages. Cross lines on the symbols represent deceased individuals.

Family A

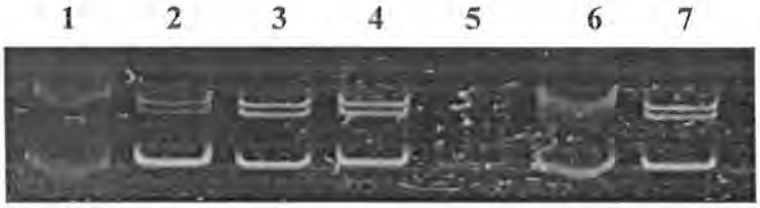

Lane 1. VI-1 Affected
Lane 2. VI-6 Affected
Lane 3. V-3 Normal
Lane 4. V-4 Normal
Lane 5. VI-5 Normal
Lane 6. VI-2 Normal
Lane 7. VI-7 Affected

Figure 3.3: Electropherogram of the ethidium bromide stained 8% non-denaturing polyacrylamide gel showing allele pattern obtained with marker D1S1665 at 104.28 cM. The Roman numerals indicate the generation number of the individuals within a pedigree while Arabic numerals indicate their positions within generation.

Family A

Lane 1. VI-1 Affected
Lane 2. VI-6 Affected
Lane 3. V-3 Normal
Lane 4. V-4 Normal
Lane 5. VI-5 Normal
Lane 6. VI-2 Normal
Lane 7. VI-7 Affected

Figure 3.4: Electropherogram of the ethidium bromide stained 8% non-denaturing polyacrylamide gel showing allele pattern obtained with marker D6S1014 at 45.50 cM. The Roman numerals indicate the generation number of the individuals within a pedigree while Arabic numerals indicate their positions within generation.

Family A

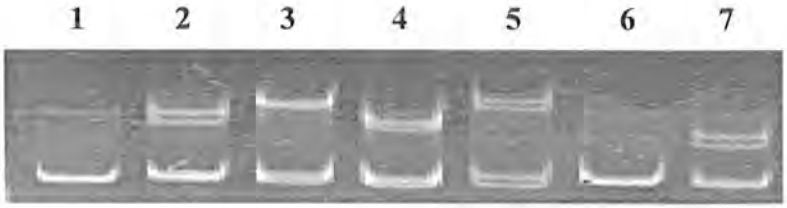

Lane 1. VI-1 Affected
Lane 2. VI-6 Affected
Lane 3. V-3 Normal
Lane 4. V-4 Normal
Lane 5. VI-5 Normal
Lane 6. VI-2 Normal
Lane 7. VI-7 Affected

Figure 3.5: Electropherogram of the ethidium bromide stained 8% non-denaturing polyacrylamide gel showing allele pattern obtained with marker GATA129G03 at 46.24 cM. The Roman numerals indicate the generation number of the individuals within a pedigree while Arabic numerals indicate their positions within generation.

Family A

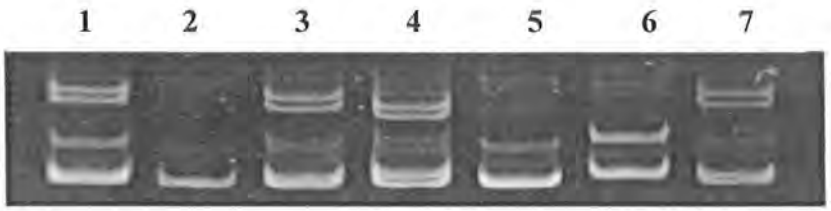

Lane 1. VI-1 Affected
Lane 2. VI-6 Affected
Lane 3. V-3 Normal
Lane 4. V-4 Normal
Lane 5. VI-5 Normal
Lane 6. VI-2 Normal
Lane 7. VI-7 Affected

Figure 3.6: Electropherogram of the ethidium bromide stained 8% non-denaturing polyacrylamide gel showing allele pattern obtained with marker D6S1031 at 93.11 cM. The Roman numerals indicate the generation number of the individuals within a pedigree while Arabic numerals indicate their positions within generation.

Family A

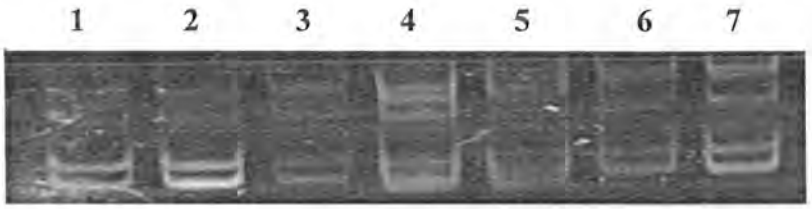

Lane 1. VI-1 Affected
Lane 2. VI-6 Affected
Lane 3. V-3 Normal
Lane 4. V-4 Normal
Lane 5. VI-5 Normal
Lane 6. VI-2 Normal
Lane 7. VI-7 Affected

Figure 3.7: Electropherogram of the ethidium bromide stained 8% non-denaturing polyacrylamide gel showing allele pattern obtained with marker D16S420 at 48.71 cM. The Roman numerals indicate the generation number of the individuals within a pedigree while Arabic numerals indicate their positions within generation.

Family A

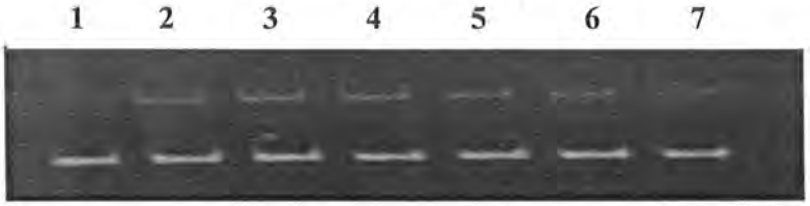

Lane 1. VI-1 Affected
Lane 2. VI-6 Affected
Lane 3. V-3 Normal
Lane 4. V-4 Normal
Lane 5. VI-5 Normal
Lane 6. VI-2 Normal
Lane 7. VI-7 Affected

Figure 3.8: Electropherogram of the ethidium bromide stained 8% non-denaturing polyacrylamide gel showing allele pattern obtained with marker D3S2316 at 131.76 cM. The Roman numerals indicate the generation number of the individuals within a pedigree while Arabic numerals indicate their positions within generation.

Family A

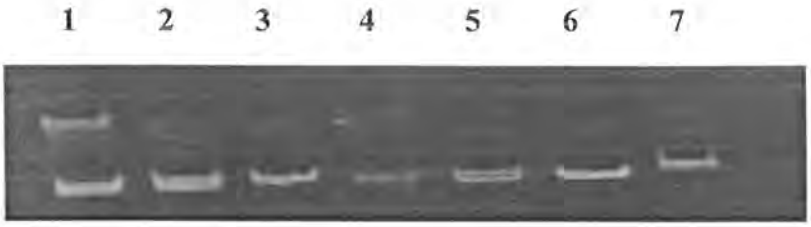

Lane 1. VI-1 Affected
Lane 2. VI-6 Affected
Lane 3. V-3 Normal
Lane 4. V-4 Normal
Lane 5. VI-5 Normal
Lane 6. VI-2 Normal
Lane 7. VI-7 Affected

Figure 3.9: Electropherogram of the ethidium bromide stained 8% non-denaturing polyacrylamide gel showing allele pattern obtained with marker D3S2322 at 140.05 cM. The Roman numerals indicate the generation number of the individuals within a pedigree while Arabic numerals indicate their positions within generation.

Family A

Lane 1. VI-1 Affected
Lane 2. VI-6 Affected
Lane 3. V-3 Normal
Lane 4. V-4 Normal
Lane 5. VI-5 Normal
Lane 6. VI-2 Normal
Lane 7. VI-7 Affected

Figure 3.10: Electropherogram of the ethidium bromide stained 8% non-denaturing polyacrylamide gel showing allele pattern obtained with marker D14S122 at 5.03 cM. The Roman numerals indicate the generation number of the individuals within a pedigree while Arabic numerals indicate their positions within generation.

Family A

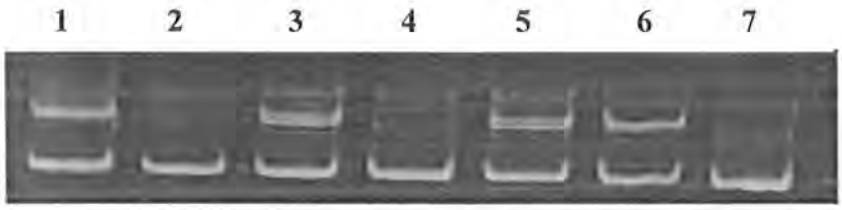

Lane 1. VI-1 Affected
Lane 2. VI-6 Affected
Lane 3. V-3 Normal
Lane 4. V-4 Normal
Lane 5. VI-5 Normal
Lane 6. VI-2 Normal
Lane 7. VI-7 Affected

Figure 3.11: Electropherogram of the ethidium bromide stained 8% non-denaturing polyacrylamide gel showing allele pattern obtained with marker D14S742 at 9.22 cM. The Roman numerals indicate the generation number of the individuals within a pedigree while Arabic numerals indicate their positions within generation.

Family A

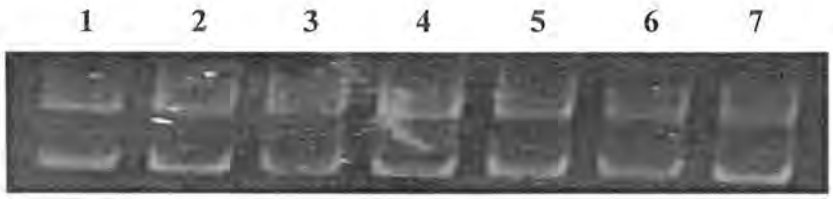

Lane 1. VI-1 Affected
Lane 2. VI-6 Affected
Lane 3. V-3 Normal
Lane 4. V-4 Normal
Lane 5. VI-5 Normal
Lane 6. VI-2 Normal
Lane 7. VI-7 Affected

Figure 3.12: Electropherogram of the ethidium bromide stained 8% non-denaturing polyacrylamide gel showing allele pattern obtained with marker D8S1119 at 96.45 cM. The Roman numerals indicate the generation number of the individuals within a pedigree while Arabic numerals indicate their positions within generation.

Family A

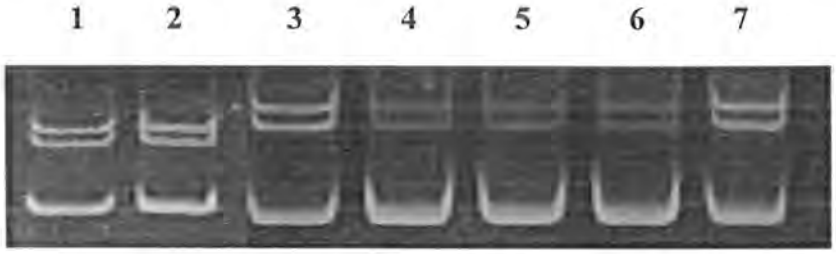

Lane 1. VI-1 Affected
Lane 2. VI-6 Affected
Lane 3. V-3 Normal
Lane 4. V-4 Normal
Lane 5. VI-5 Normal
Lane 6. VI-2 Normal
Lane 7. VI-7 Affected

Figure 3.17: Electropherogram of the ethidium bromide stained 8% non-denaturing polyacrylamide gel showing allele pattern obtained with marker D2S2972 at 116.19 cM. The Roman numerals indicate the generation number of the individuals within a pedigree while Arabic numerals indicate their positions within generation.

Family A

Lane 1. VI-1 Affected
Lane 2. VI-6 Affected
Lane 3. VII-4 Affected
Lane 4. VI-8 Normal
Lane 5. V-3 Normal
Lane 6. V-4 Normal
Lane 7. VI-5 Normal
Lane 8. VI-9 Normal
Lane 9. VI-2 Normal
Lane10 VII-3 Normal
Lane11 V-5 Affected
Lane12 V-6 Affected
Lane13 IV-7 Normal
Lane14 VII-5 Affected
Lane15 VI-7 Affected

Figure 3.18: Electropherogram of the ethidium bromide stained 8% non-denaturing polyacrylamide gel showing allele pattern obtained with marker D17S1298 at 13.24 cM. The Roman numerals indicate the generation number of the individuals within a pedigree while Arabic numerals indicate their positions within generation.

Family A

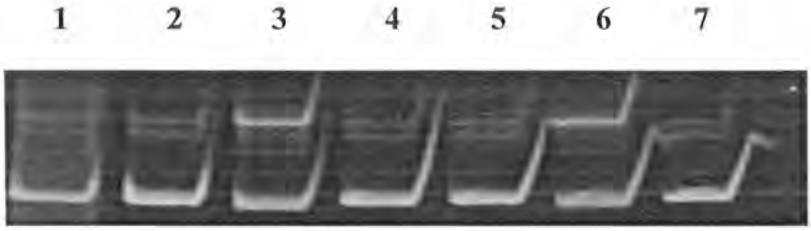

Lane 1.	VI-1	Affected	Lane 5.	VI-5	Normal
Lane 2.	VI-6	Affected	Lane 6.	VI-2	Normal
Lane 3.	V-3	Normal	Lane 7.	VI-7	Affected
Lane 4.	V-4	Normal			

Figure 3.19a: Electropherogram of the ethidium bromide stained 8% non-denaturing polyacrylamide gel showing allele pattern obtained with marker GATA158H04 at 19.97 cM. The Roman numerals indicate the generation number of the individuals within a pedigree while Arabic numerals indicate their positions within generation.

Family A

Lane 1.	VI-7	Affected	Lane 9.	VI-5	Normal
Lane 2.	VII-5	Affected	Lane10	V-4	Normal
Lane 3.	IV-7	Normal	Lane11	V-3	Normal
Lane 4.	V-6	Affected	Lane12	VI-8	Normal
Lane 5.	V-5	Affected	Lane13	VII-4	Affected
Lane 6.	VII-3	Normal	Lane14	VI-6	Affected
Lane 7.	VI-2	Normal	Lane15	VI-1	Affected
Lane 8.	VI-9	Normal			

Figure 3.19b: Electropherogram of the ethidium bromide stained 8% non-denaturing polyacrylamide gel showing allele pattern obtained with marker GATA158H04 at 19.97 cM. The Roman numerals indicate the generation number of the individuals within a pedigree while Arabic numerals indicate their positions within generation.

Family A

Lane 1.	VI-1	Affected	Lane 9.	VI-2	Normal
Lane 2.	VI-6	Affected	Lane10	VII-3	Normal
Lane 3.	VII-4	Affected	Lane11	V-5	Affected
Lane 4.	VI-8	Normal	Lane12	V-6	Affected
Lane 5.	V-3	Normal	Lane13	IV-7	Normal
Lane 6.	V-4	Normal	Lane14	VII-5	Affected
Lane 7.	VI-5	Normal	Lane15	VI-7	Affected
Lane 8.	VI-9	Normal			

Figure 3.20: Electropherogram of the ethidium bromide stained 8% non-denaturing polyacrylamide gel showing allele pattern obtained with marker D17S1805 at 24.41 cM. The Roman numerals indicate the generation number of the individuals within a pedigree while Arabic numerals indicate their positions within generation.

Family A

Lane 1.	VI-1	Affected	Lane 9.	VI-2	Normal
Lane 2.	VI-6	Affected	Lane10	VII-3	Normal
Lane 3.	VII-4	Affected	Lane11	V-5	Affected
Lane 4.	VI-8	Normal	Lane12	V-6	Affected
Lane 5.	V-3	Normal	Lane13	IV-7	Normal
Lane 6.	V-4	Normal	Lane14	VII-5	Affected
Lane 7.	VI-5	Normal	Lane15	VI-7	Affected
Lane 8.	VI-9	Normal			

Figure 3.21: Electropherogram of the ethidium bromide stained 8% non-denaturing polyacrylamide gel showing allele pattern obtained with marker D17S974 at 33.56 cM. The Roman numerals indicate the generation number of the individuals within a pedigree while Arabic numerals indicate their positions within generation.

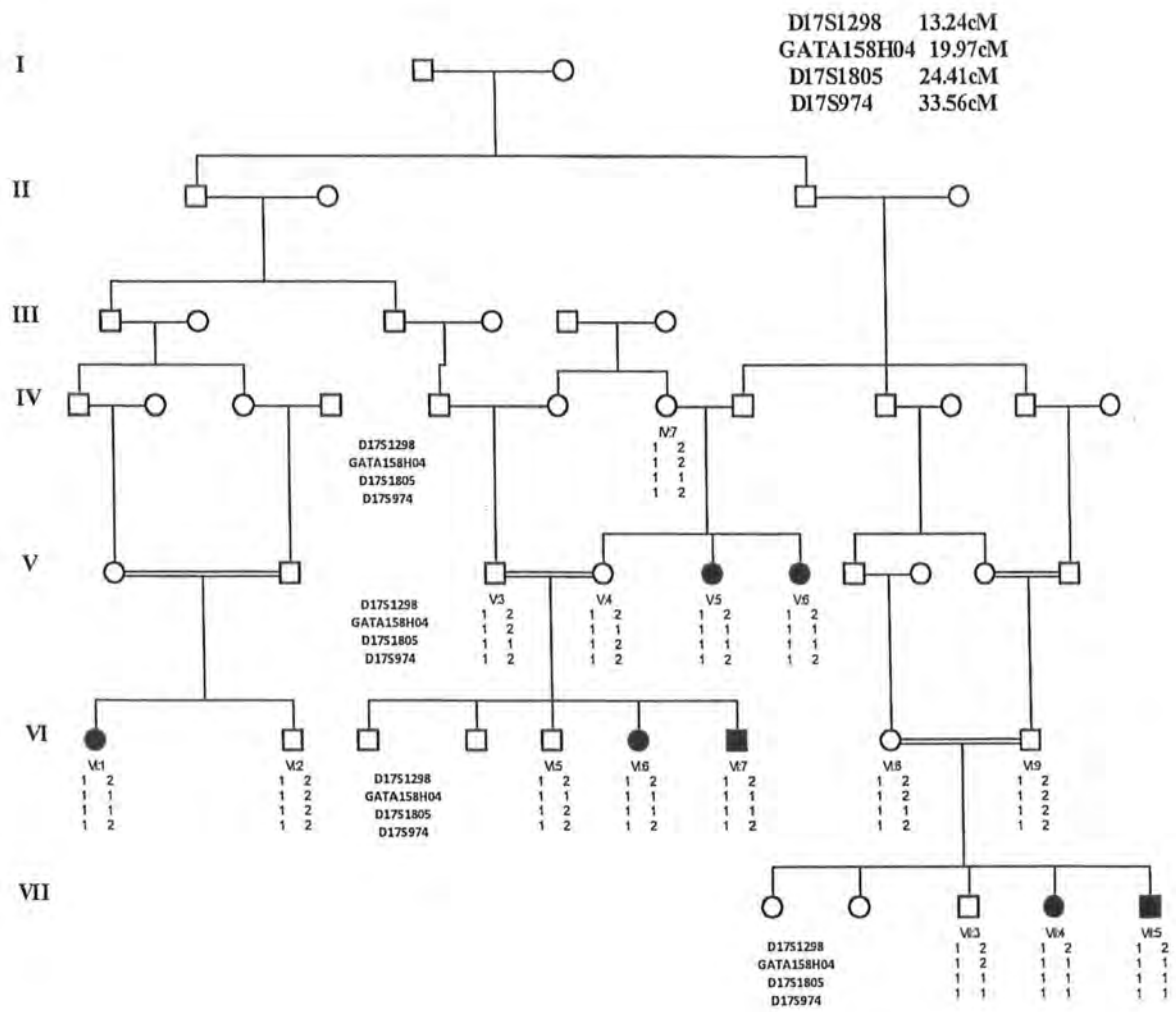

Figure 3.22: Haplotype of family A with markers showing linkage to chromosome 17p13.1

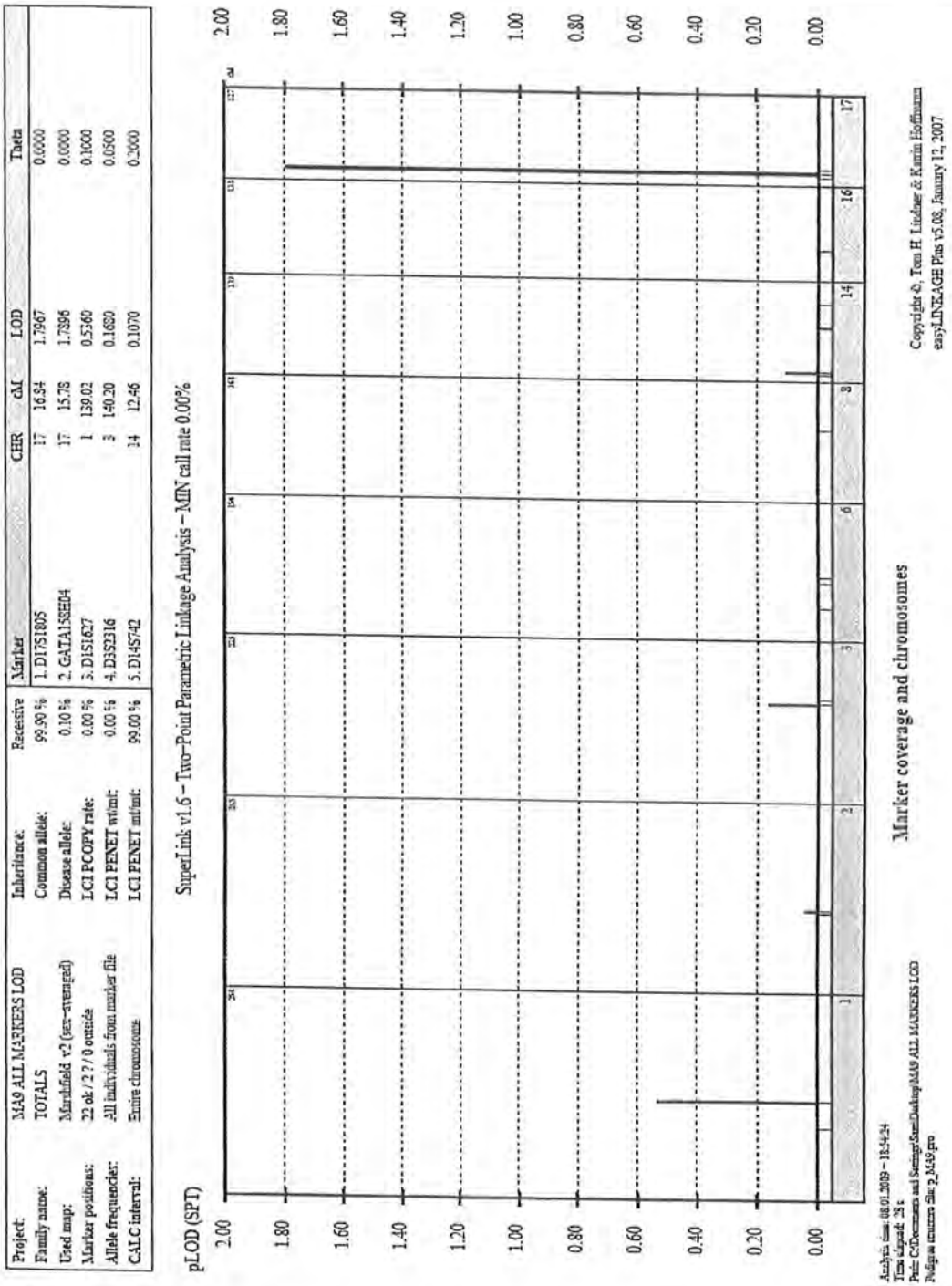

Figure 3.23: Graphical representation of LOD score calculated by easyLINKAGE plus v5.08.

Family B

Lane 1.	V-4	Affected	Lane 5.	IV-5	Affected
Lane 2.	IV-7	Normal	Lane 6.	III-2	Normal
Lane 3.	V-5	Affected	Lane 7.	III-1	Normal
Lane 4.	V-1	Normal	Lane 8.	IV-6	Normal

Figure 3.24: Electropherogram of the ethidium bromide stained 8% non-denaturing polyacrylamide gel showing allele pattern obtained with marker D1S1662 at 104.28 cM. The Roman numerals indicate the generation number of the individuals within a pedigree while Arabic numerals indicate their positions within generation.

Family B

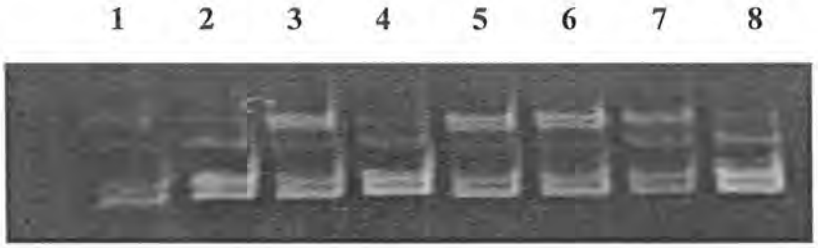

Lane 1.	V-4	Affected	Lane 5.	IV-5	Affected
Lane 2.	IV-7	Normal	Lane 6.	III-2	Normal
Lane 3.	V-5	Affected	Lane 7.	III-1	Normal
Lane 4.	V-1	Normal	Lane 8.	IV-6	Normal

Figure 3.25: Electropherogram of the ethidium bromide stained 8% non-denaturing polyacrylamide gel showing allele pattern obtained with marker D1S2876 at 108.34 cM. The Roman numerals indicate the generation number of the individuals within a pedigree while Arabic numerals indicate their positions within generation.

Family B

Lane 1. V-4 Affected
Lane 2. IV-7 Normal
Lane 3. V-5 Affected
Lane 4. V-1 Normal
Lane 5. IV-5 Affected
Lane 6. IV-4 Affected
Lane 7. III-2 Normal
Lane 8. III-1 Normal
Lane 9. IV-6 Normal

Figure 3.26: Electropherogram of the ethidium bromide stained 8% non-denaturing polyacrylamide gel showing allele pattern obtained with marker GATA129G03. The Roman numerals indicate the generation number of the individuals within a pedigree while Arabic numerals indicate their positions within generation.

Family B

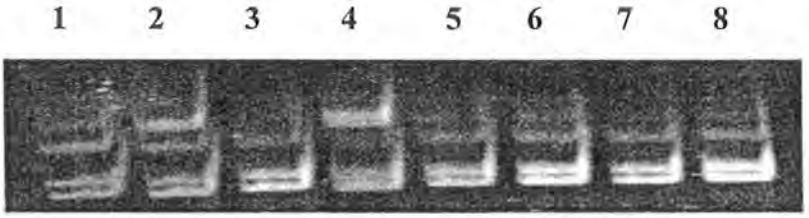

Lane 1. V-4 Affected
Lane 2. IV-7 Normal
Lane 3. V-5 Affected
Lane 4. V-1 Normal
Lane 5. IV-5 Affected
Lane 6. III-2 Normal
Lane 7. III-1 Normal
Lane 8. IV-6 Normal

Figure 3.27: Electropherogram of the ethidium bromide stained 8% non-denaturing polyacrylamide gel showing allele pattern obtained with marker D16S287 at 38.49 cM. The Roman numerals indicate the generation number of the individuals within a pedigree while Arabic numerals indicate their positions within generation.

Family B

Lane 1. V-4 Affected
Lane 2. IV-7 Normal
Lane 3. V-5 Affected
Lane 4. V-1 Normal
Lane 5. IV-5 Affected
Lane 6. III-2 Normal
Lane 7. III-1 Normal
Lane 8. IV-6 Normal

Figure 3.28: Electropherogram of the ethidium bromide stained 8% non-denaturing polyacrylamide gel showing allele pattern obtained with marker D16S420 at 48.71 cM. The Roman numerals indicate the generation number of the individuals within a pedigree while Arabic numerals indicate their positions within generation.

Family B

Lane 1. V-4 Affected
Lane 2. IV-7 Normal
Lane 3. V-5 Affected
Lane 4. V-1 Normal
Lane 5. IV-5 Affected
Lane 6. IV-4 Affected
Lane 7. III-2 Normal
Lane 8. III-1 Normal
Lane 9. IV-6 Normal

Figure 3.29: Electropherogram of the ethidium bromide stained 8% non-denaturing polyacrylamide gel showing allele pattern obtained with marker D6S1031 at 93.11cM. The Roman numerals indicate the generation number of the individuals within a pedigree while Arabic numerals indicate their positions within generation.

Family B

Lane 1.	IV-6	Normal	Lane 6.	V-1	Normal
Lane 2.	III-1	Normal	Lane 7.	V-5	Affected
Lane 3.	III-2	Normal	Lane 8.	IV-7	Normal
Lane 4.	IV-4	Affected	Lane 9.	V-4	Affected
Lane 5.	IV-5	Affected			

Figure 3.30: Electropherogram of the ethidium bromide stained 8% non-denaturing polyacrylamide gel showing allele pattern obtained with marker D6S1282 at 86.79 cM. The Roman numerals indicate the generation number of the individuals within a pedigree while Arabic numerals indicate their positions within generation.

Family B

Lane 1.	V-4	Affected	Lane 6.	IV-4	Affected
Lane 2.	IV-7	Normal	Lane 7.	III-2	Normal
Lane 3.	V-5	Affected	Lane 8.	III-1	Normal
Lane 4.	V-1	Normal	Lane 9.	IV-6	Normal
Lane 5.	IV-5	Affected			

Figure 3.31: Electropherogram of the ethidium bromide stained 8% non-denaturing polyacrylamide gel showing allele pattern obtained with marker D1S533 at 199.81 cM. The Roman numerals indicate the generation number of the individuals within a pedigree while Arabic numerals indicate their positions within generation.

Family B

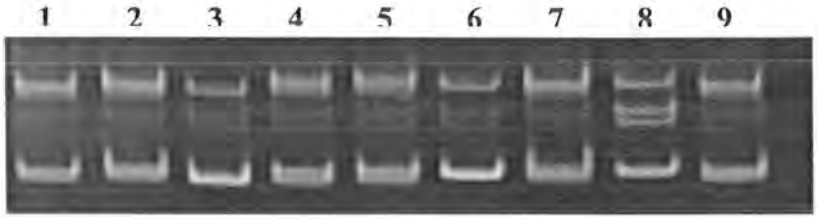

Lane 1. V-4 Affected
Lane 2. IV-7 Normal
Lane 3. V-5 Affected
Lane 4. V-1 Normal
Lane 5. IV-5 Affected
Lane 6. IV-4 Affected
Lane 7. III-2 Normal
Lane 8. III-1 Normal
Lane 9. IV-6 Normal

Figure 3.32: Electropherogram of the ethidium bromide stained 8% non-denaturing polyacrylamide gel showing allele pattern obtained with marker D1S1660 at 202.04 cM. The Roman numerals indicate the generation number of the individuals within a pedigree while Arabic numerals indicate their positions within generation.

Family B

Lane 1. V-4 Affected
Lane 2. IV-7 Normal
Lane 3. V-5 Affected
Lane 4. V-1 Normal
Lane 5. IV-5 Affected
Lane 6. IV-4 Affected
Lane 7. III-2 Normal
Lane 8. III-1 Normal
Lane 9. IV-6 Normal

Figure 3.33: Electropherogram of the ethidium bromide stained 8% non-denaturing polyacrylamide gel showing allele pattern obtained with marker D4S1548 at 152.47 cM. The Roman numerals indicate the generation number of the individuals within a pedigree while Arabic numerals indicate their positions within generation.

Family B

Lane 1. V-4 Affected
Lane 2. IV-7 Normal
Lane 3. V-5 Affected
Lane 4. V-1 Normal
Lane 5. IV-5 Affected
Lane 6. IV-4 Affected
Lane 7. III-2 Normal
Lane 8. III-1 Normal
Lane 9. IV-6 Normal

Figure 3.34: Electropherogram of the ethidium bromide stained 8% non-denaturing polyacrylamide gel showing allele pattern obtained with marker D4S3049 at 156.8 cM. The Roman numerals indicate the generation number of the individuals within a pedigree while Arabic numerals indicate their positions within generation.

Family B

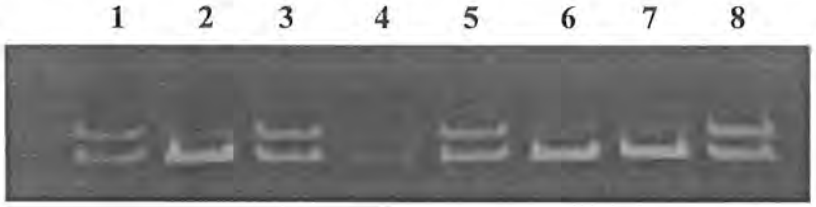

Lane 1. V-4 Affected
Lane 2. IV-7 Normal
Lane 3. V-5 Affected
Lane 4. V-1 Normal
Lane 5. IV-5 Affected
Lane 6. III-2 Normal
Lane 7. III-1 Normal
Lane 8. IV-6 Normal

Figure 3.35: Electropherogram of the ethidium bromide stained 8% non-denaturing polyacrylamide gel showing allele pattern obtained with marker D1S1588 at 122.02 cM. The Roman numerals indicate the generation number of the individuals within a pedigree while Arabic numerals indicate their positions within generation.

Family B

Lane 1.	V-4	Affected	Lane 5.	IV-5	Affected
Lane 2.	IV-7	Normal	Lane 6.	III-2	Normal
Lane 3.	V-5	Affected	Lane 7.	III-1	Normal
Lane 4.	V-1	Normal	Lane 8.	IV-6	Normal

Figure 3.36: Electropherogram of the ethidium bromide stained 8% non-denaturing polyacrylamide gel showing allele pattern obtained with marker D1S1587 at 126.2 cM. The Roman numerals indicate the generation number of the individuals within a pedigree while Arabic numerals indicate their positions within generation.

Family B

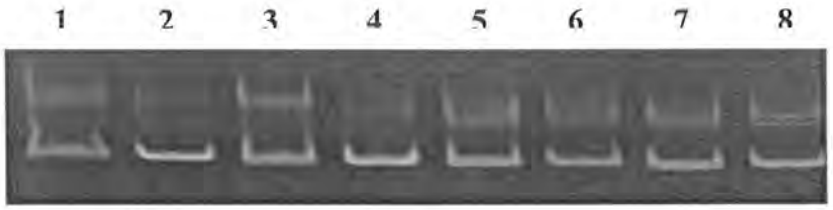

Lane 1.	V-4	Affected	Lane 5.	IV-5	Affected
Lane 2.	IV-7	Normal	Lane 6.	III-2	Normal
Lane 3.	V-5	Affected	Lane 7.	III-1	Normal
Lane 4.	V-1	Normal	Lane 8.	IV-6	Normal

Figure 3.37: Electropherogram of the ethidium bromide stained 8% non-denaturing polyacrylamide gel showing allele pattern obtained with marker D2S426 at 192.53 cM. The Roman numerals indicate the generation number of the individuals within a pedigree while Arabic numerals indicate their positions within generation.

Family B

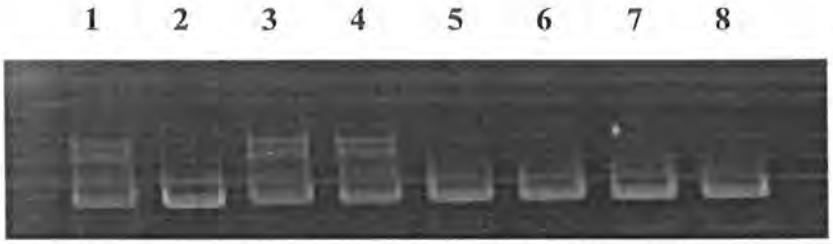

Lane 1.	V-4	Affected	Lane 5.	IV-5	Affected
Lane 2.	IV-7	Normal	Lane 6.	III-2	Normal
Lane 3.	V-5	Affected	Lane 7.	III-1	Normal
Lane 4.	V-1	Normal	Lane 8.	IV-6	Normal

Figure 3.44: Electropherogram of the ethidium bromide stained 8% non-denaturing polyacrylamide gel showing allele pattern obtained with marker D5S436 at 150.91 cM. The Roman numerals indicate the generation number of the individuals within a pedigree while Arabic numerals indicate their positions within generation.

Family B

Lane 1.	V-4	Affected	Lane 5.	IV-5	Affected
Lane 2.	IV-7	Normal	Lane 6.	III-2	Normal
Lane 3.	V-5	Affected	Lane 7.	III-1	Normal
Lane 4.	V-1	Normal	Lane 8.	IV-6	Normal

Figure 3.45: Electropherogram of the ethidium bromide stained 8% non-denaturing polyacrylamide gel showing allele pattern obtained with marker D5S812 at 155.39 cM. The Roman numerals indicate the generation number of the individuals within a pedigree while Arabic numerals indicate their positions within generation.

Family B

Lane 1.	V-4	Affected	Lane 5.	IV-5	Affected
Lane 2.	IV-7	Normal	Lane 6.	III-2	Normal
Lane 3.	V-5	Affected	Lane 7.	III-1	Normal
Lane 4.	V-1	Normal	Lane 8.	IV-6	Normal

Figure 3.46: Electropherogram of the ethidium bromide stained 8% non-denaturing polyacrylamide gel showing allele pattern obtained with marker D4S3360 at 0 cM. The Roman numerals indicate the generation number of the individuals within a pedigree while Arabic numerals indicate their positions within generation.

Family B

Lane 1.	V-4	Affected	Lane 5.	IV-5	Affected
Lane 2.	IV-7	Normal	Lane 6.	III-2	Normal
Lane 3.	V-5	Affected	Lane 7.	III-1	Normal
Lane 4.	V-1	Normal	Lane 8.	IV-6	Normal

Figure 3.47: Electropherogram of the ethidium bromide stained 8% non-denaturing polyacrylamide gel showing allele pattern obtained with marker D4S2285 at 7.97 cM. The Roman numerals indicate the generation number of the individuals within a pedigree while Arabic numerals indicate their positions within generation.

Family B

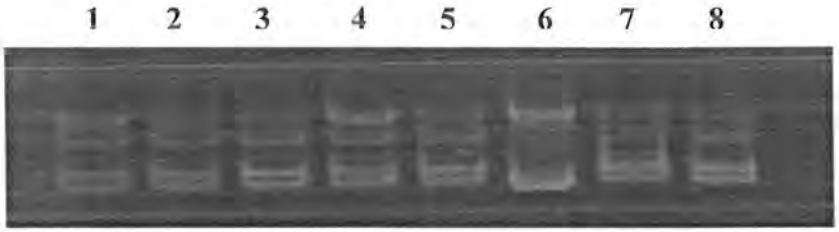

Lane 1.	V-4	Affected	Lane 5.	IV-5	Affected
Lane 2.	IV-7	Normal	Lane 6.	III-2	Normal
Lane 3.	V-5	Affected	Lane 7.	III-1	Normal
Lane 4.	V-1	Normal	Lane 8.	IV-6	Normal

Figure 3.48: Electropherogram of the ethidium bromide stained 8% non-denaturing polyacrylamide gel showing allele pattern obtained with marker D3S3607 at 135.87 cM. The Roman numerals indicate the generation number of the individuals within a pedigree while Arabic numerals indicate their positions within generation.

Family B

Lane 1.	V-4	Affected	Lane 5.	IV-5	Affected
Lane 2.	IV-7	Normal	Lane 6.	III-2	Normal
Lane 3.	V-5	Affected	Lane 7.	III-1	Normal
Lane 4.	V-1	Normal	Lane 8.	IV-6	Normal

Figure 3.49: Electropherogram of the ethidium bromide stained 8% non-denaturing polyacrylamide gel showing allele pattern obtained with marker D3S2322 at 140.05 cM. The Roman numerals indicate the generation number of the individuals within a pedigree while Arabic numerals indicate their positions within generation.

Family B

Lane 1.	V-4	Affected	Lane 5.	IV-5	Affected
Lane 2.	IV-7	Normal	Lane 6.	III-2	Normal
Lane 3.	V-5	Affected	Lane 7.	III-1	Normal
Lane 4.	V-1	Normal	Lane 8.	IV-6	Normal

Figure 3.50: Electropherogram of the ethidium bromide stained 8% non-denaturing polyacrylamide gel showing allele pattern obtained with marker D4S2290 at 104.31 cM. The Roman numerals indicate the generation number of the individuals within a pedigree while Arabic numerals indicate their positions within generation.

Family B

Lane 1.	V-4	Affected	Lane 5.	IV-5	Affected
Lane 2.	IV-7	Normal	Lane 6.	III-2	Normal
Lane 3.	V-5	Affected	Lane 7.	III-1	Normal
Lane 4.	V-1	Normal	Lane 8.	IV-6	Normal

Figure 3.51: Electropherogram of the ethidium bromide stained 8% non-denaturing polyacrylamide gel showing allele pattern obtained with marker GATA67A08. The Roman numerals indicate the generation number of the individuals within a pedigree while Arabic numerals indicate their positions within generation.

Family B

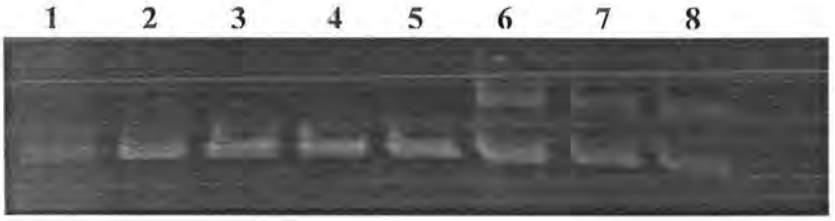

Lane 1. V-4 Affected
Lane 2. IV-7 Normal
Lane 3. V-5 Affected
Lane 4. V-1 Normal
Lane 5. IV-5 Affected
Lane 6. III-2 Normal
Lane 7. III-1 Normal
Lane 8. IV-6 Normal

Figure 3.52: Electropherogram of the ethidium bromide stained 8% non-denaturing polyacrylamide gel showing allele pattern obtained with marker D2S286 at 99.3 cM. The Roman numerals indicate the generation number of the individuals within a pedigree while Arabic numerals indicate their positions within generation.

Family B

Lane 1. V-4 Affected
Lane 2. IV-7 Normal
Lane 3. V-5 Affected
Lane 4. V-1 Normal
Lane 5. IV-5 Affected
Lane 6. IV-4 Affected
Lane 7. III-2 Normal
Lane 8. III-1 Normal
Lane 9. IV-6 Normal

Figure 3.53: Electropherogram of the ethidium bromide stained 8% non-denaturing polyacrylamide gel showing allele pattern obtained with marker D1S1627 at 134.13 cM. The Roman numerals indicate the generation number of the individuals within a pedigree while Arabic numerals indicate their positions within generation.

Family B

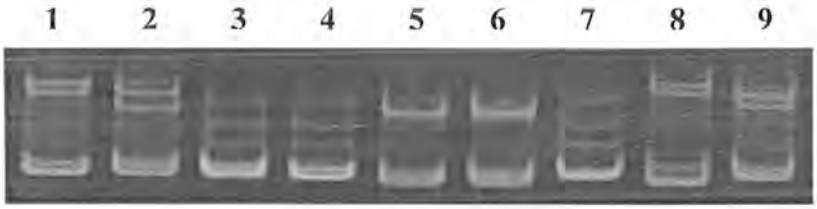

Lane 1.	V-4	Affected	Lane 6.	IV-4	Affected
Lane 2.	IV-7	Normal	Lane 7.	III-2	Normal
Lane 3.	V-5	Affected	Lane 8.	III-1	Normal
Lane 4.	V-1	Normal	Lane 9.	IV-6	Normal
Lane 5.	IV-5	Affected			

Figure 3.54: Electropherogram of the ethidium bromide stained 8% non-denaturing polyacrylamide gel showing allele pattern obtained with marker D8S1119 at 96.45 cM. The Roman numerals indicate the generation number of the individuals within a pedigree while Arabic numerals indicate their positions within generation.

Family B

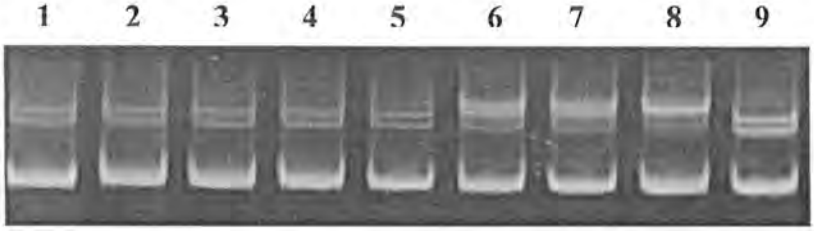

Lane 1.	V-4	Affected	Lane 6.	IV-4	Affected
Lane 2.	IV-7	Normal	Lane 7.	III-2	Normal
Lane 3.	V-5	Affected	Lane 8.	III-1	Normal
Lane 4.	V-1	Normal	Lane 9.	IV-6	Normal
Lane 5.	IV-5	Affected			

Figure 3.55: Electropherogram of the ethidium bromide stained 8% non-denaturing polyacrylamide gel showing allele pattern obtained with marker D8S1143. The Roman numerals indicate the generation number of the individuals within a pedigree while Arabic numerals indicate their positions within generation.

Family B

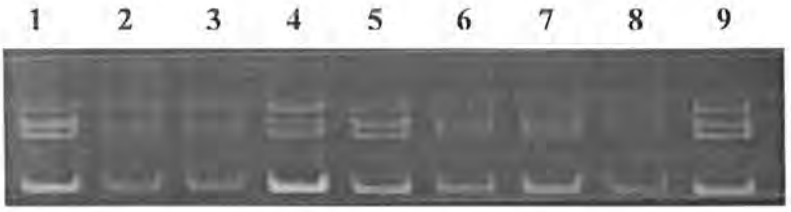

Lane 1. V-4 Affected
Lane 2. IV-7 Normal
Lane 3. V-5 Affected
Lane 4. V-1 Normal
Lane 5. IV-5 Affected
Lane 6. IV-4 Affected
Lane 7. III-2 Normal
Lane 8. III-1 Normal
Lane 9. IV-6 Normal

Figure 3.56: Electropherogram of the ethidium bromide stained 8% non-denaturing polyacrylamide gel showing allele pattern obtained with marker D2S2972 at 116.19 cM. The Roman numerals indicate the generation number of the individuals within a pedigree while Arabic numerals indicate their positions within generation.

Family B

Lane 1. V-4 Affected
Lane 2. IV-7 Normal
Lane 3. V-5 Affected
Lane 4. V-1 Normal
Lane 5. IV-5 Affected
Lane 6. IV-4 Affected
Lane 7. III-2 Normal
Lane 8. III-1 Normal
Lane 9. IV-6 Normal

Figure 3.57: Electropherogram of the ethidium bromide stained 8% non-denaturing polyacrylamide gel showing allele pattern obtained with marker D14S122 at 5.03 cM. The Roman numerals indicate the generation number of the individuals within a pedigree while Arabic numerals indicate their positions within generation.

Family B

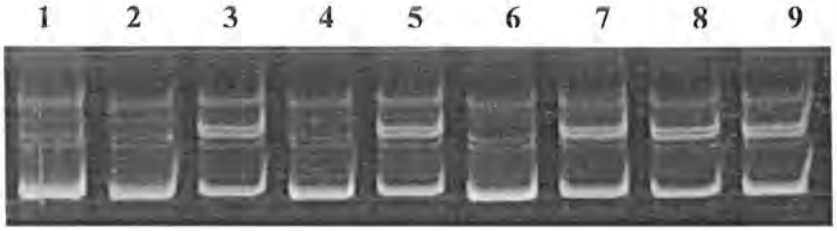

Lane 1. V-4 Affected
Lane 2. IV-7 Normal
Lane 3. V-5 Affected
Lane 4. V-1 Normal
Lane 5. IV-5 Affected
Lane 6. IV-4 Affected
Lane 7. III-2 Normal
Lane 8. III-1 Normal
Lane 9. IV-6 Normal

Figure 3.58: Electropherogram of the ethidium bromide stained 8% non-denaturing polyacrylamide gel showing allele pattern obtained with marker D14S548 at 9.22 cM. The Roman numerals indicate the generation number of the individuals within a pedigree while Arabic numerals indicate their positions within generation.

Family B

Lane 1. V-4 Affected
Lane 2. IV-7 Normal
Lane 3. V-5 Affected
Lane 4. V-1 Normal
Lane 5. IV-5 Affected
Lane 6. IV-4 Affected
Lane 7. III-2 Normal
Lane 8. III-1 Normal
Lane 9. IV-6 Normal

Figure 3.59: Electropherogram of the ethidium bromide stained 8% non-denaturing polyacrylamide gel showing allele pattern obtained with marker D19S246 at 82.48 cM. The Roman numerals indicate the generation number of the individuals within a pedigree while Arabic numerals indicate their positions within generation.

Family B

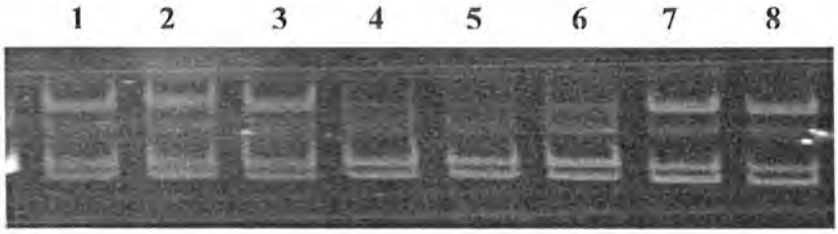

Lane 1. V-4 Affected
Lane 2. IV-7 Normal
Lane 3. V-5 Affected
Lane 4. V-1 Normal
Lane 5. IV-5 Affected
Lane 7. III-2 Normal
Lane 8. III-1 Normal
Lane 9. IV-6 Normal

Figure 3.60: Electropherogram of the ethidium bromide stained 8% non-denaturing polyacrylamide gel showing allele pattern obtained with marker D14S1069 at 62.99 cM. The Roman numerals indicate the generation number of the individuals within a pedigree while Arabic numerals indicate their positions within generation.

Family B

Lane 1. V-4 Affected
Lane 2. IV-7 Normal
Lane 3. V-5 Affected
Lane 4. V-1 Normal
Lane 5. IV-5 Affected
Lane 6. IV-4 Affected
Lane 7. III-2 Normal
Lane 8. III-1 Normal
Lane 9. IV-6 Normal

Figure 3.61: Electropherogram of the ethidium bromide stained 8% non-denaturing polyacrylamide gel showing allele pattern obtained with marker D14S588 at 64.65 cM. The Roman numerals indicate the generation number of the individuals within a pedigree while Arabic numerals indicate their positions within generation.

Family B

Lane 1. V-4 Affected
Lane 2. IV-7 Normal
Lane 3. V-5 Affected
Lane 4. V-1 Normal
Lane 5. IV-5 Affected
Lane 6. IV-4 Affected
Lane 7. III-2 Normal
Lane 8. III-1 Normal
Lane 9. IV-6 Normal

Figure 3.62: Electropherogram of the ethidium bromide stained 8% non-denaturing polyacrylamide gel showing allele pattern obtained with marker D17S1298 at 13.24 cM. The Roman numerals indicate the generation number of the individuals within a pedigree while Arabic numerals indicate their positions within generation.

Family B

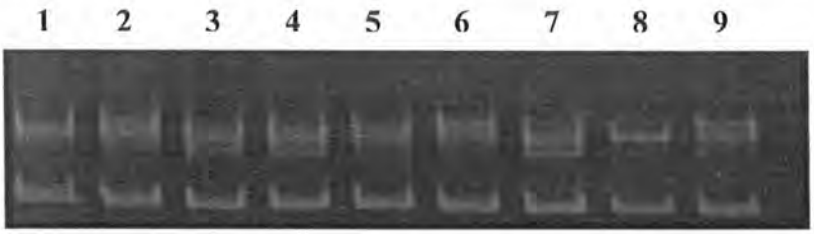

Lane 1. V-4 Affected
Lane 2. IV-7 Normal
Lane 3. V-5 Affected
Lane 4. V-1 Normal
Lane 5. IV-5 Affected
Lane 6. IV-4 Affected
Lane 7. III-2 Normal
Lane 8. III-1 Normal
Lane 9. IV-6 Normal

Figure 3.63: Electropherogram of the ethidium bromide stained 8% non-denaturing polyacrylamide gel showing allele pattern obtained with marker GATA158H04 at 19.97 cM. The Roman numerals indicate the generation number of the individuals within a pedigree while Arabic numerals indicate their positions within generation.

Family B

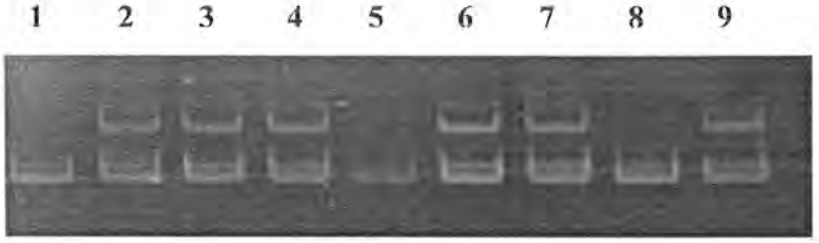

Lane 1. V-4 Affected
Lane 2. IV-7 Normal
Lane 3. V-5 Affected
Lane 4. V-1 Normal
Lane 5. IV-5 Affected
Lane 6. IV-4 Affected
Lane 7. III-2 Normal
Lane 8. III-1 Normal
Lane 9. IV-6 Normal

Figure 3.64: Electropherogram of the ethidium bromide stained 8% non-denaturing polyacrylamide gel showing allele pattern obtained with marker D17S1805 at 24.41 cM. The Roman numerals indicate the generation number of the individuals within a pedigree while Arabic numerals indicate their positions within generation.

Family B

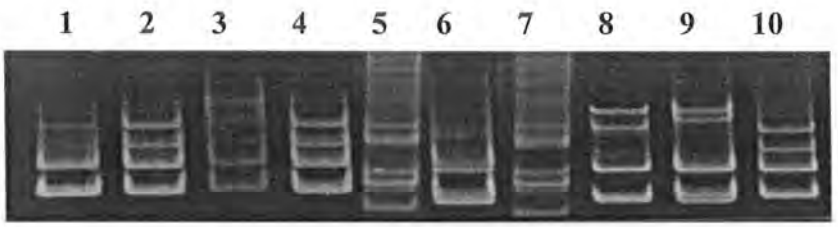

Lane 1. V-4 Affected
Lane 2. IV-7 Normal
Lane 3. V-5 Affected
Lane 4. V-1 Normal
Lane 5. V-3 Normal
Lane 6. IV-5 Affected
Lane 7. IV-4 Affected
Lane 8. III-2 Normal
Lane 9. III-1 Normal
Lane10 IV-6 Normal

Figure 3.65: Electropherogram of the ethidium bromide stained 8% non-denaturing polyacrylamide gel showing allele pattern obtained with marker D10S523 at 105.84 cM. The Roman numerals indicate the generation number of the individuals within a pedigree while Arabic numerals indicate their positions within generation.

Family B

Lane 1.	IV-7	Normal	Lane 6.	IV-5	Affected
Lane 2.	V-4	Affected	Lane 7.	IV-4	Affected
Lane 3.	V-5	Affected	Lane 8.	III-2	Normal
Lane 4.	V-1	Normal	Lane 9.	III-1	Normal
Lane 5.	V-3	Normal	Lane10	IV-6	Normal

Figure 3.66: Electropherogram of the ethidium bromide stained 8% non-denaturing polyacrylamide gel showing allele pattern obtained with marker D10S1658 at 105.38 cM. The Roman numerals indicate the generation number of the individuals within a pedigree while Arabic numerals indicate their positions within generation.

Family B

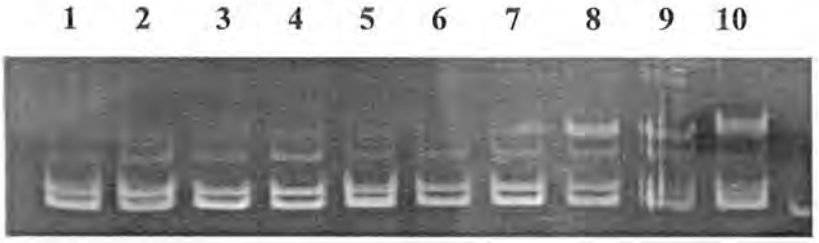

Lane 1.	V-4	Affected	Lane 6.	IV-5	Affected
Lane 2.	IV-7	Normal	Lane 7.	IV-4	Affected
Lane 3.	V-5	Affected	Lane 8.	III-2	Normal
Lane 4.	V-1	Normal	Lane 9.	III-1	Normal
Lane 5.	V-3	Normal	Lane10	IV-6	Normal

Figure 3.67: Electropherogram of the ethidium bromide stained 8% non-denaturing polyacrylamide gel showing allele pattern obtained with marker D10S1765 at 107.81 cM. The Roman numerals indicate the generation number of the individuals within a pedigree while Arabic numerals indicate their positions within generation.

Family B

Lane 1.	V-4	Affected	Lane 6.	IV-5	Affected
Lane 2.	IV-7	Normal	Lane 7.	IV-4	Affected
Lane 3.	V-5	Affected	Lane 8.	III-2	Normal
Lane 4.	V-1	Normal	Lane 9.	III-1	Normal
Lane 5.	V-3	Normal	Lane10	IV-6	Normal

Figure 3.68: Electropherogram of the ethidium bromide stained 8% non-denaturing polyacrylamide gel showing allele pattern obtained with marker D10S1143 at 109.56 cM. The Roman numerals indicate the generation number of the individuals within a pedigree while Arabic numerals indicate their positions within generation.

Family B

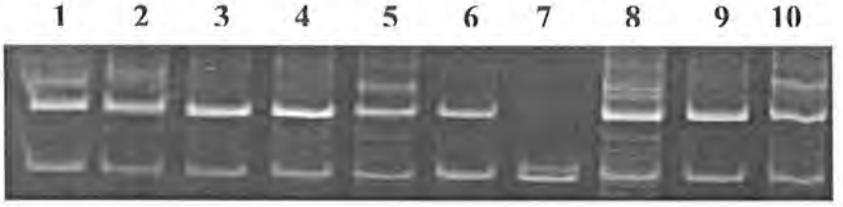

Lane 1.	V-4	Affected	Lane 6.	IV-5	Affected
Lane 2.	IV-7	Normal	Lane 7.	IV-4	Affected
Lane 3.	V-5	Affected	Lane 8.	III-2	Normal
Lane 4.	V-1	Normal	Lane 9.	III-1	Normal
Lane 5.	V-3	Normal	Lane10	IV-6	Normal

Figure 3.69: Electropherogram of the ethidium bromide stained 8% non-denaturing polyacrylamide gel showing allele pattern obtained with marker D10S1687 at 107.16 cM. The Roman numerals indicate the generation number of the individuals within a pedigree while Arabic numerals indicate their positions within generation.

Family B

Lane 1.	V-4	Affected	Lane 6.	IV-5	Affected
Lane 2.	IV-7	Normal	Lane 7.	IV-4	Affected
Lane 3.	V-5	Affected	Lane 8.	III-2	Normal
Lane 4.	V-1	Normal	Lane 9.	III-1	Normal
Lane 5.	V-3	Normal	Lane10	IV-6	Normal

Figure 3.70: Electropherogram of the ethidium bromide stained 8% non-denaturing polyacrylamide gel showing allele pattern obtained with marker D10S1644 at 105.84 cM. The Roman numerals indicate the generation number of the individuals within a pedigree while Arabic numerals indicate their positions within generation.

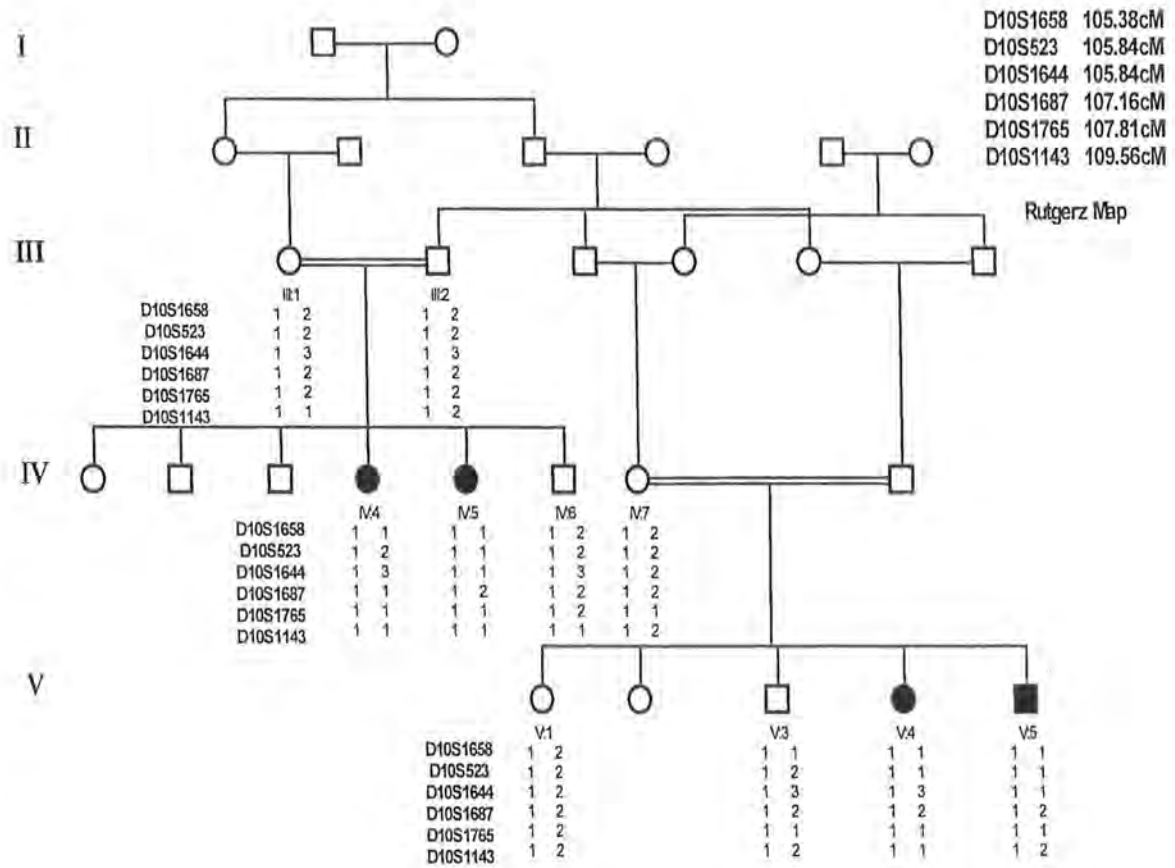

Figure 3.71: Haplotype of family B of markers showing linkage to chromosome 10q23.1

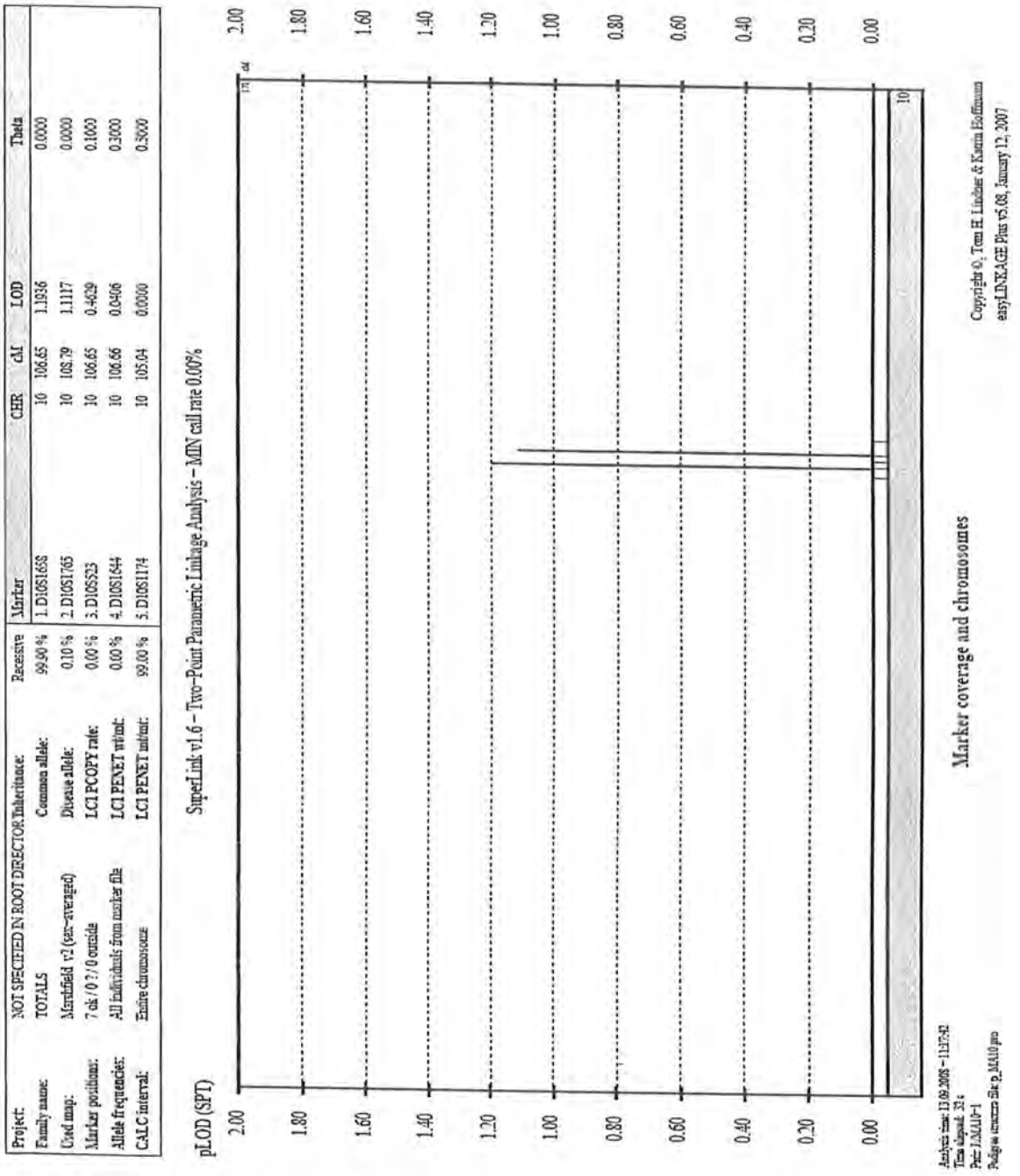

Figure 3.72: Graphical representation of LOD scores calculation using easyLINKAGE plus v5.08

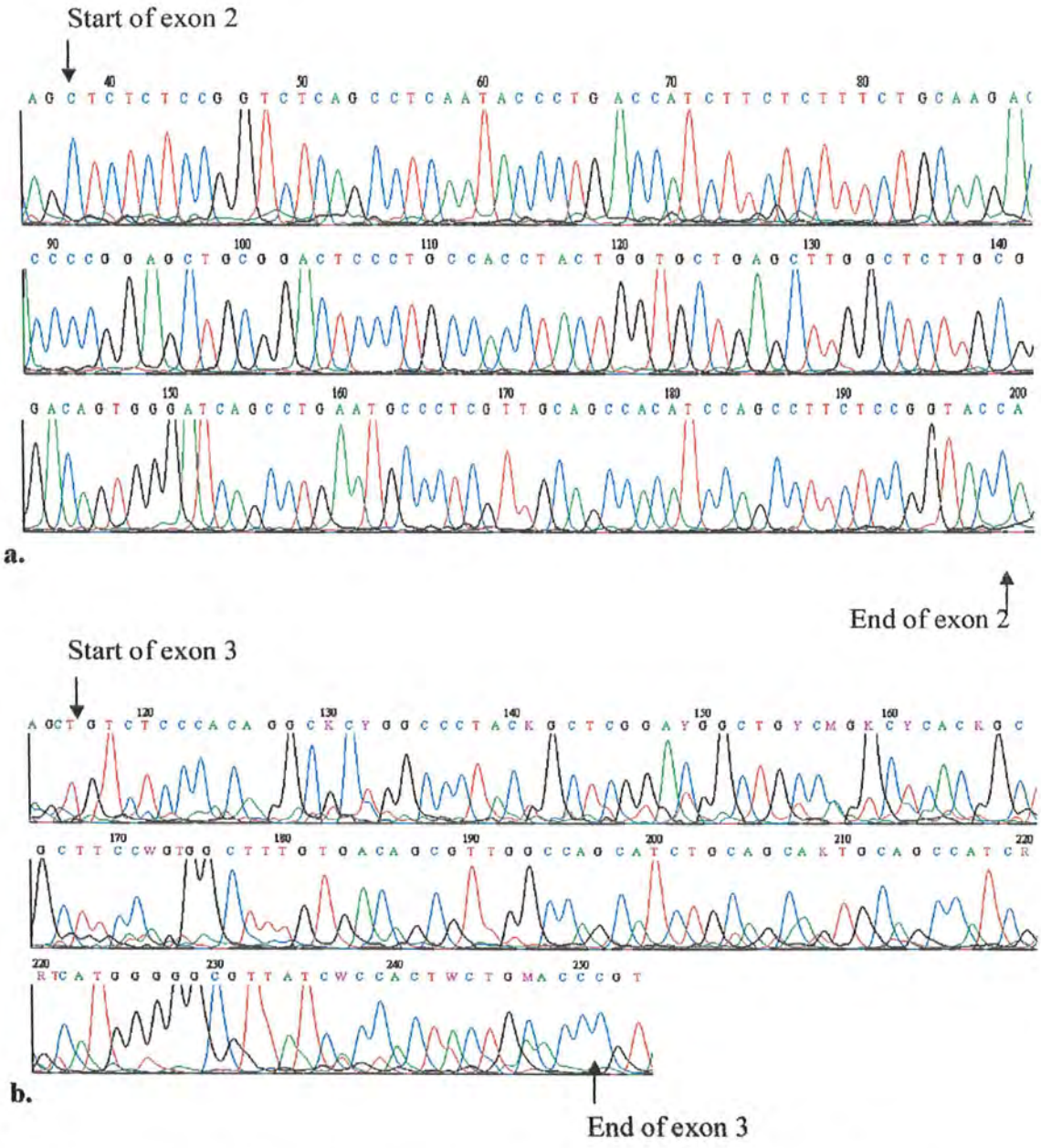

Figure 3.73: (a) Sequence chromatogram of exon 2 and **(b)** exon 3 of RGR gene

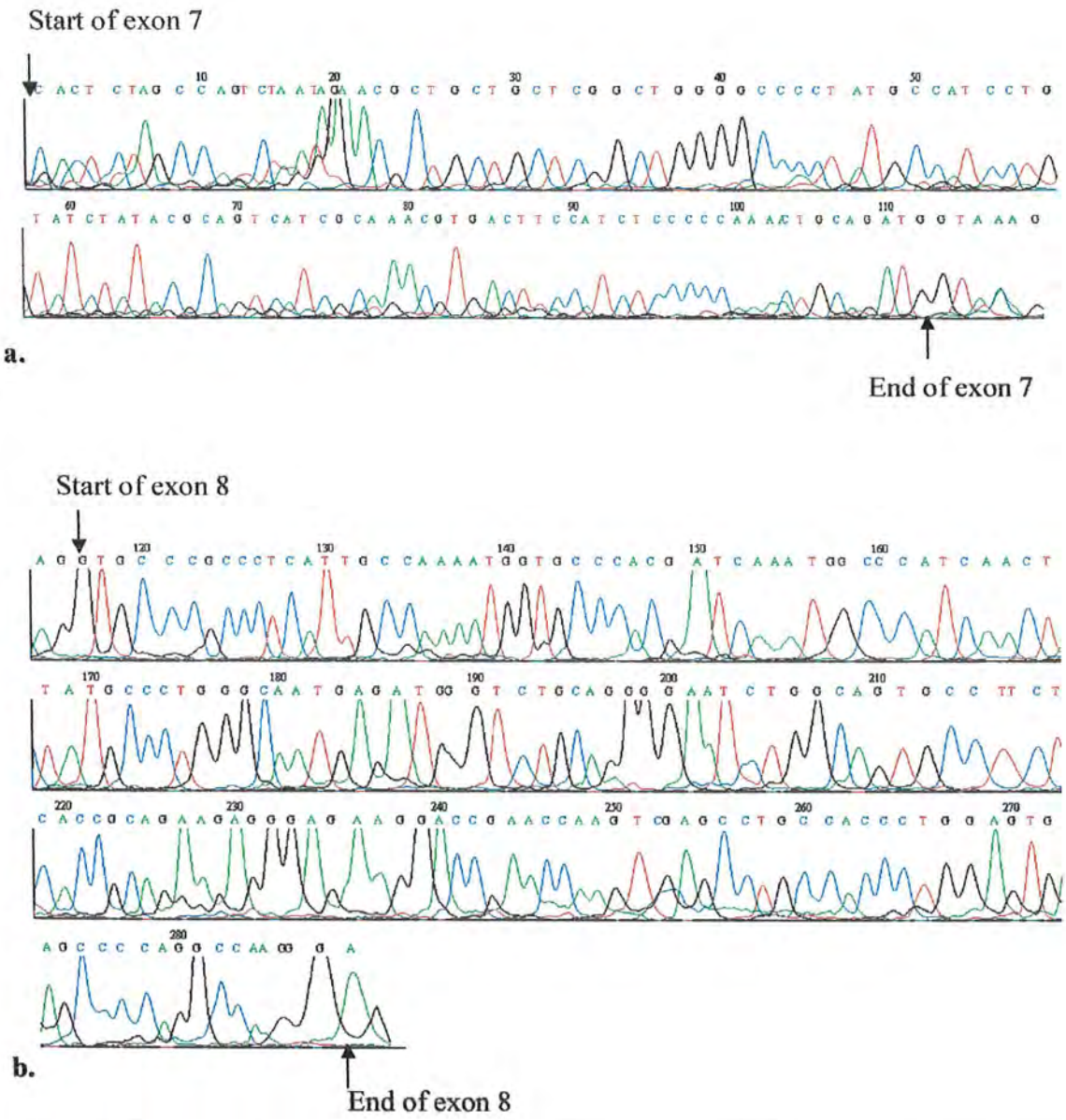

Figure 3.74: (a) Sequence chromatogram of exon 7 and **(b)** exon 8 of RGR gene

DISCUSSION

Inherited eye disorders are characterized by immense clinical and genetic heterogeneity which poses great challenges for gene identification, mutation analysis, genetic counseling, and the development of therapies. Many diseases in this group cause visual loss because of the premature death of the rod and cone photoreceptor cells. Inherited eye disorders are of special concern when they affect children i.e. congenital eye disorders because blindness in children affects their development, education and employment opportunities. Prevalence of these diseases is more in consanguineous marriages because of offspring inheriting identical ancestral genomic segments from their parents increasing the incidence of recessive disease within these sibships (Woods *et al.*, 2006; Khan *et al.*, 2007; den Hollander *et al.*, 2008).

Among various inherited eye disorders most common cause of visual impairment are the hereditary retinal diseases representing a broad range of retinal dysfunction and/or degenerations including retinitis pigmentosa, cone or cone-rod dystrophy and Leber congenital amaurosis etc. Over one hundred genes have been reported to be associated with these diseases and mutations in many different genes may cause the same disease or vice versa (Sullivan and Daiger, 1996; Zhang *et al.*, 2005a). These diseases are genetically complex and the boundaries separating some of the diagnostic categories are not distinct. Retinal dystrophies may lead to photoreceptor death or dysfunction and blindness. The majority of genes causing retinal disorders are retina specific but other genes that are ubiquitously expressed may also cause retinal phenotype (Blackshaw *et al.*, 2001; Rivolta *et al.*, 2002; Patel *et al.*, 2007).

Among the inherited retinal disorders retinitis pigmentosa (RP) is the most common retinal degeneration that is clearly hereditary. It affects about one in 5000 individuals worldwide. Patients with RP lose vision because of the death of both rods and cones throughout the retina. If the rods and cones (or perhaps other essential types of retinal neurons) are lost within the first years of life, or if they are already dead or nonfunctional at birth, the diagnosis becomes congenital retinal blindness, also referred to as Leber

congenital amaurosis, the most severe form of inherited retinal blindness which in most cases is inherited in an autosomal recessive (ar) manner (Rivolta *et. al.*, 2002; den Hollander *et al.*, 2008). The genetic basis of congenital eye and orbit anomalies is just beginning to be delineated, and future research on the subject will undoubtedly broaden understanding of the developmental etiology, pathophysiology, and treatment of congenital ocular disorders (Guercio and Martyn, 2007).

In the present study, two consanguineous Pakistani families (A and B), demonstrating hereditary congenital blindness have been ascertained from different regions of Pakistan. The mode of inheritance in these families was autosomal recessive. The affected individuals of these families showed typical features of hereditary eye disorders characterized by visual impairment with bilateral nystagmus and excessive blinking in sunlight since childhood. Dull macular refraction was present with grossly normal retina.

To identify the causative genes underlying different types of hereditary eye disorders in the families presented here, a classical linkage analysis approach called "Homozygosity Mapping" was followed. Smith (1953) indicated that offsprings of consanguineous matings are homozygous for genetic markers located near the diseased gene. Lander and Botstein, (1987) reasoned that recessive gene could be mapped using the offsprings of consanguineous unions in an approach they called "Homozygosity Mapping", which provides a rapid mean of mapping autosomal recessive gene in consanguineous families by identifying chromosomal regions that show homozygous identity-by-descend (IBD) segment in pooled samples (Miano *et al.*, 2000). In affected children of such union, a region of many centi-Morgans (cM) spanning the disease locus is almost always homozygous by descent. Other regions will also be homozygous by descent, but these regions will vary from one child to the next. The homozygosity mapping will revolve around the identification/detection of this homozygous region among all the affected individuals. The minimum detectable length of a homozygous segment depends on marker density of screening set and their heterozygosity (Broman and Weber, 1999).

In order to identify causative genes in the studied families, cosegregation and homozygosity analysis were performed with microsatellite markers corresponding to candidate genes involved in eye disorders and related phenotypes (Table 2.1 and 2.2). A minimum of two microsatellite markers from each of the candidate regions of these loci was genotyped in all the available individuals of the two families (A and B). In both families (A and B), linkage was established to the known autosomal recessive eye disorders loci on chromosome 17p13.1 and 10q23.1 respectively.

The locus mapped in case of family A contains two genes AIPL1 and GUCY2D (Khaliq *et al.,* 2002). So mutation can be present in one of these two genes. But as none of the 17p13.1 linked Pakistani families that had been reported so far, had disease associated mutations in the GUCY2D gene (Jabeen *et al.,* 2005), so sequencing of gene AIPL1 was carried out for mutation analysis. The LCA phenotypes are highly variable and change with age, and the phenotypes associated with the currently known LCA genes overlap. In case of family A the affected individuals showed dull macular refraction with grossly normal retina and the retinal phenotype of patients with AIPL1 mutations is also that of a severe, congenital retinal dystrophy with a notable maculopathy. The retinal appearances range from near normal to severely atrophic with marked maculopathy and pigmentary retinopathy. Macular involvement as seen on ophthalmoscopy likely begins with an indistinct dull or irregular foveal reflex and progresses to a diffuse ill-defined area of retinal pigment stippling and atrophy, leading to a marked atrophic maculopathy (Dharmaraj *et al.,* 2004). So phenotype of affected individuals also relates the family A to AIPL1 gene although some clinical phenotype may differ but the phenotypes of congenital blindness vary depending on the mutation and also with age.

Aryl hydrocarbon-interacting protein-like 1 (AIPL1), maps within 2.5 megabases (Mb) of GUCY2D on 17p13 and is the fourth gene to be associated with LCA (Sohocki *et al.,* 2000b). The AIPL1 gene consists of 6 exons and encodes a protein of 384 amino acids (Dharmaraj *et al.,* 2004). AIPL1 mutations may cause approximately 20% of recessive LCA. The mutations in this gene have been reported to cause retinitis pigmentosa, cone-rod dystrophy and Leber congenital dystrophy (Entrez gene,

http://www.ncbi.nlm.nih.gov/entrez). According to retina international mutation data base approximately 21 mutations and variations are so far reported (Retina international, www.sph.uth.tmc.edu) whereas in Pakistani population p.Trp278X in AIPL1 may be the founder mutation (Sohocki *et al.*, 2000b).

The sequencing results of the gene AIPL1 revealed some variation but further analysis do not suggest any pathogenic mutations that may be causing eye disorders in family A. So these results suggest that there may be a mutation in the regulatory regions of AIPL1 gene or GUCY2D gene that also maps in the region of homozygosity identified in affected individuals of family A. This would be the first time that AIPL1 do not contain any mutation, as so far all Pakistani families linked to this region have been found to contain mutations in AIPL1 gene and not the GUCY2D gene, as reported by Jabeen *et al.*, (2005).

Human gene retinal G protein-coupled receptor (RGR) was first localized by Chen *et al.*, (1996) to chromosome 10q23 which encodes an opsin protein in Müller cells and the retinal pigment epithelium (Chen *et al.*, 1996). First mutation in this gene was reported by Morimura *et al.*, (1999), but since than all reported mutations in RGR gene are associated with retinitis pigmentosa (Fong *et al.*, 2006). But this gene has never been associated with inherited congenital eye disorders. Further it has never been reported to be associated with retinitis pigmentosa in any case in Pakistan. But there are several genes which cause different eye disorders depending on the mutations which results in different functional abnormalities causing different inherited eye disorders for example CRB1 is responsible for a distinctive form of autosomal recessive RP referred to as RP12 and is also associated with LCA. Two other LCA associated genes RPE65 and TULP1 are also known to cause some cases of RP (Lotery *et al.*, 2001). A novel splice-site mutation of TULP1, c.1495+2_1495+3insT causes' autosomal recessive severe early-onset retinitis pigmentosa (RP) and also novel 6-base in-frame duplication causes Leber congenital amaurosis (Mataftsi *et al.*, 2007; Abbasi *et al.*, 2008). Based on this information, RGR gene was sequenced in family B.

The sequencing results of RGR gene in the family B revealed that exons 2 and 7 have no mutation or variation. While exon 3 and 8 have variations but further analysis revealed their non-pathogenic nature. As these polymorphism were not detected in rest of the affected family members of the family B. The disease causing mutation may be present in remaining exons of RGR gene. Identification of mutation in family B will expand the clinical representation of retinal dystrophies, as till now RGR mutations are responsible for RP.

The discovery of inherited eye disorder genes and mutations will help to understand the functional outcomes of these mutations and their relation to the phenotype of the disease resulting in a better knowledge of development and progression of inherited eye disorders. Genetic tests utilizing mutation analysis in causative genes of various inherited eye disorders may be used for carrier detection and diagnosis but due to heterogeneity of these disorders it is not yet possible but this may help our future generations to develop new therapeutics and diagnostic tools for the cure of inherited eye disorders. Many other complex disorders which may have overlapping gene pathways with inherited eye disorder may in turn be able to be better understood. This will only be possible if we collect a very large genotypic database from different populations and cultures and identified all the loci and the genes involved in the disease pathogenesis towards which the present study is a small but handy contribution.

REFERENCE

- Abbasi AH, Garzozi HJ, Ben-Yosef T (2008). A novel splice-site mutation of TULP1 underlies severe early-onset retinitis pigmentosa in a consanguineous Israeli Muslim Arab family. Mol Vis 14:675-682
- Ahmed E, Loewenstein J (2008). Leber congenital amaurosis: disease, genetics and therapy. Semin Ophthalmol 23(1):39-43
- Awater H, Kerlin JR, Evans KK, Tong F (2005). Cortical representation of space around the blind spot. J Neurophysiol 94:3314-3324
- Ayyagari R, Demirci FY, Liu J, Bingham EL, Stringham H, Kakuk LE, Boehnke M, Gorin MB, Richards JE, Sieving PA (2002). X-linked recessive atrophic macular degeneration from RPGR mutation. Genomics 80:166-171
- Bainbridge JWB, Smith AJ, Barker SS, Robbie S, Henderson R, Balaggan K, Viswanathan A, Holder GE, Stockman A, Tyler N, Petersen-Jones S, Bhattacharya SS, Thrasher AJ, Fitzke FW, Carter BJ, Rubin GS, Moore AT, Ali RR (2008). Effect of gene therapy on visual function in Leber's congenital amaurosis. N Engl J Med 358:1-9
- Bennett RL, Stelnhaus KA, Uhrich SB, O'Sullivan CK, Resta RG, Lochner-Doyle D, Markel DS, Vincent V, Hamanishi J (1995). Recommendations for standardized human pedigree nomenclature. Am J Hum Genet 56:745-752
- Bergen AA, Pinckers AJLG (1997). Localization of a novel X-linked progressive cone dystrophy gene to Xq27: evidence for genetic heterogeneity. Am J Hum Genet 60(6):1468-1473
- Bessant DAR, Payne AM, Snow BE, Antiñolo G, Mehdi SQ, Bird AC, Siderovski DP, Bhattacharya SS (2000). Importance of the autosomal recessive retinitis pigmentosa locus on 1q31-q32.1 (RP12) and mutation analysis of the candidate gene RGS16 (RGS-r). J Med Genet 37:384-387
- Black MM and Sonksen PM (1992). Congenital retinal dystrophies: a study of early cognitive and visual development. Arch Disea Child 67:262-265

- Blackshaw S, Fraioli RE, Furukawa T, Cepko CL (2001). Comprehensive analysis of photoreceptor gene expression and the identification of candidate retinal disease genes. Cell 107:579-589
- Booij JC, Florijn RJ, ten Brink JB, Loves W, Meire F, van Schooneveld MJ, de Jong PTVM, Bergen AAB (2005). Identification of mutations in the AIPL1, CRB1, GUCY2D, RPE65, and RPGRIP1 genes in patients with juvenile retinitis pigmentosa. J Med Genet 42(11):67
- Brea-Fernández AJ, Pomares E, Brión MJ, Marfany G, Blanco MJ, Sánchez-Salorio M, González-Duarte R, Carracedo A (2008). Novel splice donor site mutation in MERTK gene associated with retinitis pigmentosa. British J Ophthalmo l92:1419-1423
- Broman K, Murray JC, Scheffield VC, White RL, Weber JL (1998). Comprehensive human genetics maps: individual and sex specific variation in recombination. Am J Hum Genet 63:861-869
- Broman KW, Weber KW (1999). Long homozygous chromosomal segments in the CEPH families. Am J Hum Genet 65:1493-1500
- Camuzat A, Dollfus H, Rozet JM, Gerber S, Bonneau D, Bonnemaison M, Briard ML, Dufier JL, Ghazi I, Leowski C (1995). A gene for Leber's congenital amaurosis maps to chromosome 17p. Hum Mol Genet 4(8):1447-52
- Chen XN, Korenberg JR, Jiang M, Shen D, Fong HKW (1996). Localization of the human RGR opsin gene to chromosome 10q23. Hum Genet 97:720-722
- Chen Y, Moiseyev G, Takahashi Y, Ma JX (2006). Impacts of two point mutations of RPE65 from Leber's congenital amaurosis on the stability, subcellular localization and isomerohydrolase activity of RPE65. FEBS Letters 580:4200-4204
- Cremers FPM, van de Pol DJR, van Driel M, den Hollander AI, van Haren FJJ, Knoers NVAM, Tijmes N, Bergen AAB, Rohrschneider K, Blankenagel A, Pinckers AJLG, Deutman AF, Hoyng CB (1998). Autosomal recessive retinitis

pigmentosa and cone–rod dystrophy caused by splice site mutations in the Stargardt's disease gene ABCR. Hum Mol Genet 7(3):355-362

- Cremers M, van den Hurk JAJ, den Hollander AI (2002). Molecular genetics of Leber congenital amaurosis. Hum Mol Genet 11:1169-1176
- Demirci FYK, Rigatti BW, Wen G, Radak AL, Mah TS, Baic CL, Traboulsi EI, Alitalo T, Ramser J, Gorin MB (2002). X-linked cone-rod dystrophy (locus COD1): identification of mutations in RPGR exon ORF15. Am J Hum Genet 70(4):1049-1053
- den Hollander AI, Koenekoop RK, Mohamed MD, Arts HH, Boldt K, Towns KV, Sedmak T, Beer M, Nagel-Wolfrum K, McKibbin M, Dharmaraj S, Lopez I, Ivings L, Williams GA, Springell K, Woods CG, Jafri H, Rashid Y, Strom TM, van der Zwaag B, Gosens I, Kersten FFJ, van Wijk E, Veltman JA, Zonneveld MN, van Beersum SEC, Maumenee IH, Wolfrum U, Cheetham ME, Ueffing M, Cremers FPM, Inglehearn CF, Roepman R (2007). Mutations in LCA5, encoding the ciliary protein lebercilin, cause Leber congenital amaurosis. Nat Genet 39(7):889-895
- den Hollander AI, Koenekoop RK, Yzer S, Lopez I, Arends ML, Voesenek KEJ, Zonneveld MN, Strom TM, Meitinger T, Brunner HG, Hoyng CB, van den Born LI, Rohrschneider K, Cremers FPM (2006). Mutations in the CEP290 (NPHP6) gene are a frequent cause of Leber congenital amaurosis. Am J Hum Genet 79:556-561
- den Hollander AI, Roepman R, Koenekoop RK, Cremers FPM (2008). Leber congenital amaurosis: genes, proteins and disease mechanisms. Prog Retinal Eye Res 27:391-419
- Dharmaraj S, Leroy BP, Sohocki MM, Koenekoop RK, Perrault I, Anwar K, Khaliq S, Devi RS, Birch DG, De Pool E, Izquierdo N, Van Maldergem L, Ismail M, Payne AM, Holder GE, Bhattacharya SS, Bird AC, Kaplan J, Maumenee IH (2004). The phenotype of Leber congenital amaurosis in patients with AIPL1 mutations. Arch Ophthalmol 122:1029-1037

- Dharmaraj S, Leroy PB, Sohocki MM, Koenekoop RK, Perrault I, Anwar K, Khaliq S, Devi RS, Birch DG, Pool ED, Izquierdo N, Van Maldergem L, Ismail M, Payne AM, Holder GE, Bhattacharya SS, Bird AC, Kaplan J, Maumenee IH (2004). The phenotype of Leber congenital amaurosis in patients with AIPL1 mutations. Arch Ophthalmol 122:1029-1037
- Dharmaraj S, Li Y, Robitaille JM, Silva E, Zhu D, Mitchell TN, Maltby LP, Baffoe-Bonnie AB, Maumenee IH (2000). A novel locus for Leber congenital amaurosis maps to chromosome 6q. Am J Hum Genet 66(1):319-326
- Donders F (1857). Beiträge zur pathologischen Anatomie des Auges. Pigment bildung in der Netzhaut. Arch Ophthalmol 3:139-165
- Dryja TP, Adams SM, Grimsby JL, McGee TL, Hong DH, Li T, Andréasson S, Berson EL (2001). Null RPGRIP1 alleles in patients with Leber congenital amaurosis. Am J Hum Genet 68(5):1295-1298
- Farber DB, Heckenlively JR, Sparkes RS and Bateman JB (1991). Molecular genetics of retinitis pigmentosa. West J Med 155:388-399
- Farrar GJ, Kenna PF, Humphries P (2002). On the genetics of retinitis pigmentosa and on mutation-independent approaches to therapeutic intervention. EMBO J 21(5):857-864
- Feshelson M, Geiger D (2002). Exact genetic linkage computations for general pedigrees. Bioinformatics: 9 (Suppl.1):S189-S198
- Fong HKW, Lin MY, Pandey S (2006). Exon-skipping variant of RGR opsin in human retina and pigment epithelium. Exp Eye Res 83:133-140
- Freund CL, Gregory-Evans CY, Furukawa T, Papaioannou M, Looser J, Ploder L, Bellingham J, Ng D, Herbrick JA, Duncan A, Scherer SW, Tsui LC, Loutradis-Anagnostou A, Jacobson SG, Cepko CL, Bhattacharya SS, McInnes RR (1997). Cone-rod dystrophy due to mutations in a novel photoreceptor-specific homeobox gene (CRX) essential for maintenance of the photoreceptor. Cell 91 (4):543-53
- Gerber S, Perrault I, Hanein S, Barbet F, Ducroq D, Ghazi I, Coignard DM, Leowski C, Homfray T, Dufier JL, Munnich A, Kaplan J, Rozet JM (2001). Complete exon-intron structure of the RPGR-interacting protein (RPGRIP1) gene

allows the identification of mutations underlying Leber congenital amaurosis. Euro J Hum Genet 9:561-571.

- Golczak M, Imanishi M, Kuksa V, Maeda T, Kubota R, Palczewski K (2005). Lecithin: Retinol acyltransferase is responsible for amidation of retinylamine, a potent inhibitor of the retinoid cycle. J Biol Chem 280(51):42263-42273
- Goodwin P (2008). Hereditary retinal disease. Curr Opin Ophthalmol 19(3):255-62
- Graw J (2003). The genetic and molecular basis of congenital eye defects. Nat Rev Genetics 4:876-888
- Gregory-Evans K, Bhattacharya SS (1998). Genetic blindness: current concepts in the pathogenesis of human outer retinal dystrophies. Trends Genet 14:103-108
- Guercio JR, Martyn LJ (2007). Congenital malformations of the eye and orbit. Otolaryngol Clin North Am 40(1):113-40
- Hall TA, (1999). BioEdit: a user-friendly biological sequence alignment editor and analysis program for Windows 95/98/NT. Nucl Acids Symp Ser 41:95-98
- Hameed A, Khaliq S, Ismail M, Anwar K, Ebenezer ND, Jordan T, Mehdi SQ, Payne AM, Bhattacharya SS (2000). A novel locus for Leber congenital amaurosis (LCA4) with anterior keratoconus mapping to chromosome 17p13. Invest Ophthalmol Vis Sci 41:629-633
- Hameed A, Khaliq S, Ismail M, Anwar K, Mehdi SQ, Bessant D, Payne AM, Bhattacharya SS (2001). A new locus for autosomal recessive RP (RP29) mapping to chromosome 4q32-4q34 in a Pakistani family. Invest Ophthalmol Vis Sci 42:1436-1438
- Hamel CP (2006). Review: Retinitis pigmentosa. Orphanet J Rare Disea 1:40
- Hamel CP (2007). Cone rod dystrophies. Orphanet J Rare Disea 2:7
- Hargrave PA, McDowell JH, Curtis DR, Wang JK, Juszczak E, Fong SL, Rao JK, Argos P (1983). The structure of bovine rhodopsin. Biophys Struct Mech 9:235-244
- Hmani-Aifa H, Benzina Z, Zulfiqar F, Dhouib H, Shahzadi A, Ghorbel A, Rebaı¨ A, So¨derkvist P, Riazuddin S, Kimberling WJ, Ayadi H (2008). Identification of

two new mutations in the GPR98 and the PDE6B genes segregating in a Tunisian family. Eur J Hum Genet 1-9

- Jabeen F, Jalali S, Sultana S, Shami SA, Khaliq S, Ismail M, Abid A, Nasir M (2005). Identification of LCA4 locus in a Pakistani consanguineous kindred suffering from Leber's congenital amaurosis. Pak J Med Res 44(3):125-129
- Jadoon MZ, Dineen B, Bourne RRA, Shah SP, Khan MA, Johnson GJ, Gilbert CE, Kahn MD (2006). Prevalence of blindness and visual Impairment in Pakistan: The Pakistan national blindness and visual impairment survey. Invest Ophthalmol Vis Sci 47:4749-4755
- Jalali S, Jabeen F, Sultana S, Shami SA, Khaliq S, Ismail M, Abid A, Nasir M (2005). Identification of LCA4 locus in a Pakistani consanguineous kindred suffering from a distinct type of Leber's Congenital Amaurosis (LCA). Ann Pak Inst Med Sci 1(3):162-6
- Jalkanen R, Demirci FY, Tyynismaa H, Bech-Hansen T, Meindl A, Peippo M, Mäntyjärvi M, Gorin MB, Alitalo T (2003). A new genetic locus for X linked progressive cone-rod dystrophy. J Med Genet 40:418-423
- Keen TJ, Mohamed MD, McKibbin M, Rashid Y, Jafri H, Maumenee IH Inglehearn CF (2003). Identification of a locus (LCA9) for Leber's congenital amaurosis on chromosome 1p36. Eur J Hum Genet 11:420-423
- Khaliq S, HameedA, Abid A, Ismail M, Anwar M, Mehdi SQ (2002). A novel mutation in the AIPL1 gene associated with Leber congenital amaurosis in a Pakistani family. HGM Poster Abstracts: 7. Med Genomics: Poster No:314
- Khan SJ, Hassan A, Khalid L, Karim U Hashmi E, Gul F, Jehan I (2007). Blindness in children at the Ida Rieu School for the blind and deaf. J Pak Med Assoc 57(7):334-337
- Koenekoop RK (2004). An overview of Leber congenital amaurosis: A model to understand retinal development. Surv Ophthalmol 49(4):379-398
- Kong X, Murphy K, Raj T, He C, White PS, Matise TC (2004). A combined linkage-physical map of the human genome. Am J Hum Genet 75:1143-1148

- Kumar A, Shetty J, Kumar B, Blanton SH (2004). Confirmation of linkage and refinement of the RP28 locus for autosomal recessive retinitis pigmentosa on chromosome 2p14-p15 in an Indian family. Mol Vis 10:399-402
- Lander ES, Botstein D (1987). Homozygosity mapping: a way to map human recessive traits with the DNA of inbred children. Sci 236(4808):1567-1570
- Leber T (1869). Uber retinitis pigmentosa and angeborene amaurose. Graefes Arch Klin Exp Ophthalmol 15:1-25
- Leutelt J, Oehlmann R, Younus F, van den Born LI, Weber JL, Denton MJ, Mehdi SQ, Gal A (1995). Autosomal recessive retinitis pigmentosa locus maps on chromosome 1q in a large consanguineous family from Pakistan. Clin Genet 47(3):122-4
- Linder TH, Hoffman K (2005). easyLINKAGE: A PERL script for easy and automated two/multi-point linkage analysis. Bioinformatics 21:405-407
- Lodish H, Bark A, Zipursky SL, Matsudaira P, Baltimore D, Darnell J (2002). Molecular cell biology. 4th ed. WH Freeman and company, USA
- Lorenz B, Gyurus P, Preising M, Bremser D, Gu, S, Andrassi M, Gerth C, Gal A (2000). Early onset severe rod–cone dystrophy in young children with RPE65 mutations. Invest Ophthalmol Vision Sci 41:2735-2742
- Lotery AJ, Jacobson SG, Fishman GA, Weleber RG, Fulton AB, Namperumalsamy P, He´on E, Levin AV, Grover S, Rosenow JR, Kopp KK, Sheffield VC, Stone EM (2001). Mutations in the CRB1 gene cause Leber congenital amaurosis. Arch Ophthalmol 119:415-420
- Lotery AJ, Namperumalsamy P, Jacobson SG, Weleber RG, Fishman GA, Musarella MA, Hoyt CS, H!eon E, Levin A, Jan J, Lam B, Carr RE, Franklin A, Radha S, Andorf JL, Sheffield VC, Stone EM (2000). Mutation analysis of 3 genes in patients with Leber congenital amaurosis. Arch Ophthalmol 118:538-543
- Mataftsi A, Schorderet DF, Chachoua L, Boussalah M, Nouri MT, Barthelmes D, Borruat FX, Munier FL (2007). Novel TULP1 mutation causing Leber congenital amaurosis or early onset retinal degeneration. Invest Ophthalmol Vis Sci 48:5160-5167

- Maubaret C, Hamel C (2005). Genetics of retinitis pigmentosa: metabolic classification and phenotype/genotype correlations. J Fr Ophtalmol 28(1):71-92
- Meindl A, Dry K, Herrmann K, Manson E, Ciccodicola A, Edgar A, Carvalho MRS, Achatz H, Hellebrand H, Lennon A, Migliaccio C, Porter K, Zrenner E, Bird A, Jay M, Lorenz B, Wittwer B, D'Urso D, Meitinger T, Wright A (1996). A gene (RPGR) with homology to the RCC1 guanine nucleotide exchange factor is mutated in X−linked retinitis pigmentosa (RP3). Nat Genet 13:35-42
- Miano MG, Jacobson SG, Carothers A, Hanson I, Teague P, Lovell J, Cideciyan AV, Haider N, Stone EM, Sheffield VC, Wright AF (2000). Pitfalls in homozygosity mapping. Am J Hum Genet 67:1348-1351
- Michaelides M, Hardcastle AJ, Hunt DM, Moore AT (2006). Progressive cone and cone-rod dystrophies: phenotypes and underlying molecular genetic basis. Surv Ophthalmol 51:232-258
- Mohamed MD, Topping NC, Jafri H, Raashed Y, McKibbin MA, Inglehearn CF (2003). Progession of phenotype in Leber's congenital amaurosis with a mutation at the LCA5 locus. Brit J Ophthalmol 87:473-475
- Morimura H, Fishman GA, Grover SA, Fulton AB, Berson EL, Dryja TP (1998). Mutations in the RPE65 gene in patients with autosomal recessive retinitis pigmentosa or Leber congenital amaurosis. Proc Natl Acad Sci USA 95:3088-3093
- Morimura H, Saindelle-Ribeaudeau F, Berson EL, Dryja TP (1999). Mutations in RGR, encoding a light-sensitive opsin homologue, in patients with retinitis pigmentosa. Nature Genetics 23:393-394
- O'Connell JR, Weeks DE (1998). Ped Check: a program for identification of genotype incompatibilities in linkage analysis. Am J Hum Genet 63:256-259
- Pagon RA, Daiger SP (2005). Gene Review: Retinitis Pigmentosa Overview. Gene Reviews University of Washington, Seattle.
- Patel N, Adewoyin T, Chong NV (2007). Age-related macular degeneration: a perspective on genetic studies. Eye 22:768-776

- Perrault I, Rozet JM, Ghazi I, Leowski C, Bonnemaison M, Geber S, Ducroq D, Cabot A, Souied E, Dufier JL, Munnich A, Kaplan J (1999). Different functional outcome of RetGC1 and RPE65 gene mutations in Leber congenital amaurosis. Am J Hum Genet 64:1225-1228
- Ramprasad VL, Soumittra N, Nancarrow D, Sen P, McKibbin M, Williams GA, Arokiasamy T, Lakshmipathy P, Inglehearn CF, Kumaramanickavel G (2008). Identification of a novel splice-site mutation in the Lebercilin (LCA5) gene causing Leber congenital amaurosis. Mol Vis 14:481-486.
- Riazuddin SA, Zulfiqar F, Zhang Q, Yao W, Li S, Jiao X, Shahzadi A, Amer M, Iqbal M, Hussnain T, Sieving PA, Riazuddin S, Hejtmancik JF (2006). Mutations in the gene encoding the α-subunit of rod phosphodiesterase in consanguineous Pakistani families. Mol Vis 12:1283-1291
- Riuz A, Borrege S, Marcos I, Antiñolo G (1998). A major locus for autosomal recessive retinitis pigmentosa on 6q, determined by homozygosity mapping of chromosomal regions that contain gamma-amino butyric acid-receptor clusters. Am J Hum Genet 62:1452-1459
- Rivolta C, Sharon D, DeAgelis MM, Dryja TP (2002). Retinitis pigmentosa and allied diseases: numerous diseases, genes, and inheritance patterns. Hum Mol Genet 11:10 1219-1227
- Roepman R, van Duijnhoven G, Rosenberg T, Pinckers AJLG, Bleeker-Wagemakers LM, Bergen AAB, Post J, Beck A, Reinhardt R, Ropers HH, Cremers FPM, Berger W (1996). Positional cloning of the gene for X-linked retinitis pigmentosa 3: homology with the guanine-nucleotide exchange factor RCC1. Hum Mole Genet 5(7):1035-1041
- Seeliger MW, Biesalski HK, Wissinger B, Gollnick H, Gielen S, Frank J, Beck S, Zrenner E (1999). Phenotype in retinol deficiency due to a hereditary defect in retinol binding protein synthesis. Invest Ophthalmol Vis Sci 40:3-11
- Seong MW, Kim SY, Yu YS, Hwang JM, Kim JY, Park SS (2008). Molecular characterization of Leber congenital amaurosis in Koreans. Mol Vis 14:1429-1436

- Shu X, BlackGC, Rice JM, Hart-Holden N, Jones A, O'Grady A, Ramsden S, Wright AF (2007). Mutation update: RPGR mutation analysis and disease: An update. Hum Mut 0:1-7
- Simovich MJ, Miller B, Ezzeldin H, Kirkland BT, McLeod G, Fulmer C, Nathans J, Jacobson SG, Pittler SJ (2001). Four novel mutations in the RPE65 gene in patients with Leber congenital amaurosis. Hum Mutat 18:164
- Smith C (1953). The detection of linkage in human genetics. J Royal Stat Soc B 15:153-184
- Sohocki MM, Bowne SJ, Sullivan LS, Blackshaw S, Cepko, CL, Payne, AM, Bhattacharya SS, Khaliq S, Mehdi SQ, Birch DG, Harrison WR, Elder FFB, Heckenlively JR, Daiger SP (2000a). Mutations in a new photoreceptor pineal gene on 17p cause Leber congenital amaurosis. Nat Genet 24:79-83
- Sohocki MM, Perrault I, Leroy BP, Payne AM, Dharmaraj S, Bhattacharya SS, Kaplan J, Maumenee IH, Koenekoop R, Meire FM, Birch DG, Heckenlively JR, Daiger SP (2000b). Prevalence of AIPL1 mutations in inherited retinal degenerative disease. Mol Genet Metab 70:142-150
- Sohocki MM, Sullivan LS, Mintz-Hittner HA, Birch D, Heckenlively JR, Freund CL, McInnes RR, Daiger SP (1998). A range of clinical phenotypes associated with mutations in CRX, a photoreceptor transcription-factor gene. Am J Hum Genet 63:1307-1315
- Stone EM (2007). Leber congenital amaurosis-a model for efficient genetic testing of heterogeneous disorders: LXIV Edward Jackson Memorial Lecture. Am J Ophthalmol 144:791-811
- Sullivan LS, Daiger SP (1996). Inherited retinal degeneration: exceptional genetic and clinical heterogeneity. Mol Med Today 2:380-386
- Swaroop A, Wang QL, Wu W, Cook J, Coats C, Xu S, Chen S, Zack DJ, Sieving PA (1999). Leber congenital amaurosis caused by a homozygous mutation (R90W) in the homeodomain of the retinal transcription factor CVRX: direct evidence for the involvement of CRX in the development of photoreceptor function. Hum Mol Genet 8(2):299-305

- Thompson DA, Gal A (2003). Vitamin A metabolism in the retinal pigment epithelium: genes, mutations, and diseases. Prog Retinal Eye Res 22:683-703
- Thompson DA, Janecke AR, Lange J, Feathers KL, Hubner CA, McHenry CL, Stockton DW, Rammesmayer G, Lupski JR, Antinolo G, Ayuso C, Baiget M, Gouras P, Heckenlively JR, den Hollander A, Jacobson SG, Lewis RA, Sieving PA, Wissinger B, Yzer S, Zrenner E, Utermann G, Gal A (2005). Retinal degeneration associated with RDH12 mutations results from decreased 11-cis retinal synthesis due to disruption of the visual cycle. Hum Mol Genet 14(24):3865-75
- Thompson DA, Li Y, McHenry CL, Carlson TJ, Ding X, Sieving PA, Apfelstedt-Sylla E, Gal A (2001). Mutations in the gene encoding lecithin retinol acyltransferase are associated with early-onset severe retinal dystrophy. Nat Genet 28(2):123-4
- Travis GH, Golczak M, Moise AR, Palczewski K (2007). Diseases caused by defects in the visual cycle: retinoids as potential therapeutic agents. Annu Rev Pharmacol Toxicol 47:469-512
- Tucker CL, Ramamurthy V, Pina AL, Loyer M, Dharmaraj S, Li Y, Maumenee IH, Hurley JB, Koenekoop RK (2004). Functional analyses of mutant recessive GUCY2D alleles identified in Leber congenital amaurosis patients: protein domain comparisons and dominant negative effects. Mol Vis 10:297-303
- Tuson M, Marfany G, Gonza'lez-Duarte R (2004). Mutation of CERKL, a novel human ceramide kinase gene, causes autosomal recessive retinitis pigmentosa (RP26). Am J Hum Genet. 74:128–138
- Vallespin E, Cantalapiedra D, Riveiro-Alvarez R, Wilke R, Aguirre-Lamban J, Avila-Fernandez A, Lopez-Martinez MA, Gimenez A, Trujillo-Tiebas MJ, Ramos C, Ayuso C (2007). Mutation screening of 299 Spanish families with retinal dystrophies by Leber congenital amaurosis genotyping microarray. Invest Ophthalmol Vis Sci 48:5653-5661
- Van der Spuy J, Chapple JP, Clark BJ, Luthert PJ, Sethi CS, Cheetham ME (2002). The Leber congenital amaurosis gene product AIPL1 is localized

exclusively in Rod photoreceptors of the adult human retina. Hum Mol Genet 11(7): 823-831

- Van der Spuy J, Kim JH, Yu YS, Szel A, Luthert PJ, Clark BJ, Cheetham ME (2003). The expression of the Leber congenital amaurosis protein AIPL1 coincides with rod and cone photoreceptor development. Invest Ophthalmol Vis Sci 44:5396-5403
- Vervoort R, Lennon A, Bird AC, Tulloch B, Axton R, Miano MG, Meindl A, Meitinger T,Ciccodicola A, Wright AF (2000). Mutational hot spot within a new RPGR exon in X-linked retinitis pigmentosa. Nat Genet 2000 25(4):462-6
- Walia S, Fishman GA, Zernant-Rajang J, Raime K, Allikmets R (2008). Phenotypic expression of a PRPF8 gene mutation in a Large African American family. Arch Ophthalmol 126(8):1127-32
- Wang DY, Chan WM, Tam POS, Baum L, Lam DSC, Chong KKL, Pang CP (2005a). Gene mutations in retinitis pigmentosa and their clinical implications. Clinica Chimica Acta 351:5-16
- Wang DY, Chan WM, Tam POS, Chiang SWY, Lam DSC, Chong KKL, Pang CP (2005b). Genetic markers for retinitis pigmentosa. Hong kong Med J 11: 281-288
- Weleber RG, Francis PJ and Trzupek KM (2006). GeneReviews: Leber congenital amaurosis. Gene Reviews University of Washington, Seattle.
- Woods CG, Cox J, Springell K, Hampshire DJ, Mohamed MD, Mckibbin M, Starn R, Raymond FL, Sandford R, Sharif SM, Karbani G, Ahmed M, Bond J, Clayton D, Inglehearn CF (2006). Quantification of homozygosity in consanguineous individuals with autosomal recessive disease. Am J Hum Genet 78: 889-896
- Yang Z, Peachey NS, Moshfeghi DM, Thirumalaichary S, Chorich L, Shugart YY, Fan K, Zhang K (2002). Mutations in the RPGR gene cause X-linked cone dystrophy. Hum Mol Genet 11(5):605-611
- Yzer S, Fishman GA, Racine J, Al-Zuhaibi S, Chakor H, Dorfman A, Szlyk J, Lachapelle P, van den Born LI, Allikmets R, Lopez I, Cremers FPM, Koenekoop

RK (2006). CRB1 heterozygotes with regional retinal dysfunction: implications for genetic testing of Leber congenital amaurosis. Invest Ophthalmol Vis Sci 47(9):3736-3744

- Zernant J, Ku¨lm M, Dharmaraj S, den Hollander AI, Perrault I, Preising MN, Lorenz B, Kaplan J, Cremers FPM, Maumenee I, Koenekoop RK, Allikmets R (2005). Genotyping Microarray (Disease Chip) for Leber Congenital Amaurosis: Detection of Modifier Alleles. Invest Ophthalmol Vis Sci 46:3052-3059
- Zhang Q, Zulfiqar F, Riazuddin SA, Xiao X, Ahmad Z, Riazuddin S, Hejtmancik JF, (2004). Autosomal recessive retinitis pigmentosa in a Pakistani family mapped to CNGA1 with identification of a novel mutation. Mol Vis 10:884-9
- Zhang Q, Zulfiqar F, Riazuddin SA, Xiao X, Yasmeen A, Rogan PK, Caruso R, Sieving PA, Riazuddin S, Hejtmancik JF (2005a). A variant form of Oguchi disease mapped to 13q34 associated with partial deletion of GRK1 gene. Mol Vis 11:977-985
- Zhang Q, Zulfiqar F, Xiao X, Riazuddin SA, Ayyagari R, Sabar F, Caruso R, Sieving PA, Riazuddin S, Hejtmancik JF (2005b). Severe autosomal recessive retinitis pigmentosa maps to chromosome 1p13.3–p21.2 between D1S2896 and D1S457 but outside ABCA4. Hum Genet 118:356-365
- Zito I, Downes SM, Patel RJ, Cheetham ME, Ebenezer ND, Jenkins SA, Bhattacharya SS, Webster AR, Holder GE, Bird AC, Bamiou DE, Hardcastle AJ (2003). RPGR mutation associated with retinitis pigmentosa, impaired hearing, and sinorespiratory infections. J Med Genet 40:609-615

Electronic Database:

- Clandinin T, 2006. Bio254 Lecture notes: Molecular and cellular neurobiology

  http://www.openwetware.org/wiki/BIO254:Phototransduction

- Disease info viewer H-InvDB (Annotated human gene database)

  http://www.jbirc.jbic.or.jp/hinv/orphan/pathology.cgi

- Ensembl Genome Browser

  http://www.ensembl.org

- Kaplan J and Rozet JM (2006). Encyclopedia of Life Sciences: Eye Disorders: Hereditary.

  www.interscience .wiley.com/emrw

- Leroy BP and Dharmaraj S (2003). Leber congenital amaurosis. Orphanet Encyclopedia.

  http://www.orpha.net/data/patho/GB/uk-LCA.pdf

- Montgomery MT, 2008. Overview: Anatomy, Physiology and Pathology of the Human Eye.

  http://www.tedmontgomery.com/the_eye/index.html

- NCBI (Entrez)

  http://www.ncbi.nlm.nih.gov/entrez/

- Retinal Information Network, RetNet

  www.sph.uth.tmc.edu/Retnet/home.htm

- Roberts D (2008). Cone-Rod Dystrophy

  http://www.mdsupport.org/

- UCSC Genome Browser

  http://genome.ucsc.edu/cgi-bin

- Wikipedia, the Free encyclopedia

  http:// www.wikipedia.org.

ANNEXURE I

Marker Representative file of Family B

MARKER	INDIVIDUAL ID	INDIVIDUAL ID	ALLELE 1	ALLELE 2
D10S1658	1	1	0	0
D10S1658	2	2	0	0
D10S1658	3	3	0	0
D10S1658	4	4	0	0
D10S1658	5	5	0	0
D10S1658	6	6	0	0
D10S1658	7	7	0	0
D10S1658	8	8	0	0
D10S1658	9	9	1	2
D10S1658	10	10	1	2
D10S1658	11	11	0	0
D10S1658	12	12	0	0
D10S1658	13	13	0	0
D10S1658	14	14	0	0
D10S1658	15	15	1	1
D10S1658	16	16	1	1
D10S1658	17	17	1	2
D10S1658	18	18	1	2
D10S1658	19	19	0	0
D10S1658	20	20	1	2
D10S1658	21	21	1	1
D10S1658	22	22	1	1
D10S1658	23	23	1	1

ANNEXURE II

Pedigree Representative file of Family B

FAMILY	INDIVIDUAL ID	FATHER ID	MOTHER ID	SEX*		STATUS*	
				M:1	F:2	N:1	A:2
FAMILY B	2	0	0	2		1	
FAMILY B	3	0	0	1		1	
FAMILY B	4	1	2	2		1	
FAMILY B	5	1	2	1		1	
FAMILY B	6	0	0	2		1	
FAMILY B	7	0	0	1		1	
FAMILY B	8	0	0	2		1	
FAMILY B	9	3	4	2		1	
FAMILY B	10	5	6	1		1	
FAMILY B	11	5	6	1		1	
FAMILY B	12	7	8	2		1	
FAMILY B	13	5	6	2		1	
FAMILY B	14	7	8	1		1	
FAMILY B	15	10	9	2		2	
FAMILY B	16	10	9	2		2	
FAMILY B	17	10	9	1		1	
FAMILY B	18	11	12	2		1	
FAMILY B	19	14	13	1		1	
FAMILY B	20	19	18	2		1	
FAMILY B	21	19	18	1		1	
FAMILY B	22	19	18	2		2	
FAMILY B	23	19	18	1		2	

*Sex: M= Male, F= Female

*Status: N= Normal, A= Affected